RESEARCH ARTICLE

Casein kinase 1ε and 1α as novel players in polycystic kidney disease and mechanistic targets for (R)-roscovitine and (S)-CR8

Katy Billot,[1] Charlène Coquil,[1] Benoit Villiers,[1] Béatrice Josselin-Foll,[2] Nathalie Desban,[2]
Claire Delehouzé,[2] Nassima Oumata,[1] Yannick Le Meur,[3] Alessandra Boletta,[4] Thomas Weimbs,[5]
Melanie Grosch,[6] Ralph Witzgall,[6] Sophie Saunier,[7] Evelyne Fischer,[8] Marco Pontoglio,[8] Alain Fautrel,[9]
Michal Mrug,[10,11] Darren Wallace,[12] Pamela V. Tran,[12,13] Marie Trudel,[14] Nikolay Bukanov,[15]
Oxana Ibraghimov-Beskrovnaya,[15] and Laurent Meijer[1]

[1]ManRos Therapeutics, Centre de Perharidy, Roscoff, France; [2]CNRS "Protein Phosphorylation and Human Disease Group, Station Biologique, Roscoff Cedex, Bretagne, France; [3]Service de Néphrologie, Centre Hospitalier Universitaire La Cavale Blanche, Rue Tanguy Prigent, Brest Cedex, France; [4]Division of Genetics and Cell Biology, DIBIT San Raffaele Scientific Institute, Milan, Italy; [5]Department of Molecular, Cellular, and Developmental Biology, Neuroscience Research Institute, University of California Santa Barbara, Santa Barbara, California; [6]University of Regensburg, Institute for Molecular and Cellular Anatomy, Universitätsstr 31, Regensburg, Germany; [7]INSERM U1163, Institut Imagine, Paris, France; [8]"Expression Génique, Développement et Maladies", Equipe 26/INSERM U1016/CNRS UMR 8104/Université Paris-Descartes, Institut Cochin, Département Génétique & Développement, Paris, France; [9]Université de Rennes 1, H2P2 Histopathology Core Facility, Rennes Cedex, France; [10]Division of Nephrology, University of Alabama at Birmingham, Birmingham, Alabama; [11]Department of Veterans Affairs Medical Center, Birmingham, Alabama; [12]University of Kansas Medical Center, The Jared Grantham Kidney Institute, Kansas City, Kansas; [13]University of Kansas Medical Center, Department of Anatomy and Cell Biology, Kansas City, Kansas; [14]Institut de Recherches Cliniques de Montréal, Molecular Genetics and Development, Montreal, Quebec, Canada; and [15]Sanofi Genzyme, Rare Renal and Bone Diseases, Framingham, Massachusetts

Billot K, Coquil C, Villiers B, Josselin-Foll B, Desban N, Delehouzé C, Oumata N, Le Meur Y, Boletta A, Weimbs T, Grosch M, Witzgall R, Saunier S, Fischer E, Pontoglio M, Fautrel A, Mrug M, Wallace D, Tran PV, Trudel M, Bukanov N, Ibraghimov-Beskrovnaya O, Meijer L. Casein kinase 1ε and 1α as novel players in polycystic kidney disease and mechanistic targets for (R)-roscovitine and (S)-CR8. *Am J Physiol Renal Physiol* 315: F57–F73, 2018. First published March 14, 2018; doi:10.1152/ajprenal.00489.2017.—Following the discovery of (R)-roscovitine's beneficial effects in three polycystic kidney disease (PKD) mouse models, cyclin-dependent kinases (CDKs) inhibitors have been investigated as potential treatments. We have used various affinity chromatography approaches to identify the molecular targets of roscovitine and its more potent analog (S)-CR8 in human and murine polycystic kidneys. These methods revealed casein kinases 1 (CK1) as additional targets of the two drugs. CK1ε expression at the mRNA and protein levels is enhanced in polycystic kidneys of 11 different PKD mouse models as well as in human polycystic kidneys. A shift in the pattern of CK1α isoforms is observed in all PKD mouse models. Furthermore, the catalytic activities of both CK1ε and CK1α are increased in mouse polycystic kidneys. Inhibition of CK1ε and CK1α may thus contribute to the long-lasting attenuating effects of roscovitine and (S)-CR8 on cyst development. CDKs and CK1s may constitute a dual therapeutic target to develop kinase inhibitory PKD drug candidates.

casein kinase 1; cyclin-dependent kinase; kinase inhibitor; polycystic kidney disease; roscovitine

INTRODUCTION

Polycystic kidney disease (PKD) is characterized by the progressive growth of fluid-filled cysts originating in renal tubules and can lead to end-stage renal disease (ESRD) (reviewed in Refs. 1, 4, 52, 76, and 78). PKD is considered a ciliopathy, i.e. a disease linked to abnormalities in the structure/functions of primary cilia (2, 36, 39, 54). Autosomal Dominant PKD (ADPKD) is among the most common life-threatening genetic disorders (occurring in 1/200–1,000 individuals worldwide). ADPKD is caused by >1,800 pathogenic mutations in the *Polycystic Kidney Disease 1* (*PKD1*) gene (78%), *PKD2* gene (15%) or other genes (7%). *PKD1* and *PKD2* encode polycystin-1 and polycystin-2, respectively. Autosomal Recessive PKD (AR-PKD) (1/20,000 individuals) results from mutations in the *PKHD1* gene, encoding fibrocystin. Besides the modestly active Tolvaptan (9) recently approved for the treatment of ADPKD, there is no effective therapy for PKD, leaving transplantation or dialysis as the only treatment once ESRD has been reached. Yet numerous novel therapies are currently under evaluation (reviewed in Refs. 49, 57, 64, and 79).

Abnormalities in protein kinase regulation and phosphorylation are associated with numerous diseases. Targeting specific kinases constitutes a major approach for the pharmaceutical industry in its search for new therapeutics. More than 250 kinase inhibitors have undergone clinical trials, and approxi-

Address for reprint requests and other correspondence: L. Meijer, ManRos Therapeutic, Centre de Perharidy, Hôtel de Recherche, Roscoff, France 29680 (e-mail: meijer@manros-therapeutics.com).

mately 37 products have reached the market (reviewed in Refs. 63 and 93–95). The discovery of the beneficial effects of the purine (R)-roscovitine (hereafter referred to as roscovitine) in three PKD mouse models ignited interest in pharmacological inhibitors of CDKs as potential anti-PKD drugs (13, 14, 39, 48, 66, 67, 85). Indeed, roscovitine induced cell cycle arrest, decreased apoptotic cell death of cystic-lining epithelial cells, and markedly reduced cystic volume and improved renal function. CDKs have been a major target in the search for specific pharmacological inhibitors because of their implication in numerous diseases, including cancers, neurodegenerative disorders, inflammation, renal diseases, and viral infections, etc. Pharmacological inhibitors of CDKs have also been evaluated in various kidney diseases such as glomerulonephritis (35, 62, 70, 80), lupus nephritis (100), collapsing glomerulopathy (32), cisplatin-induced nephrotoxicity (37, 38, 72, 73), kidney transplantation (69), and PKD (13, 14, 48, 66, 67, 85). Among the inhibitors initially developed as potential anticancer drug candidates, roscovitine is currently in phase 2 clinical evaluation against non-small cell lung, nasopharyngeal, and breast cancers, Cushing syndrome and cystic fibrosis are reviewed in Refs. 19 and 58–60. More recently a roscovitine derivative, (S)-CR8 (hereafter referred to as CR8), was found to be ~100-fold more potent at inducing tumor cell apoptosis (5, 6) and was also more potent at reducing cystogenesis in an ADPKD mouse model (13). An extensive study of the selectivity of roscovitine and CR8 showed that casein kinases 1 (CK1s), CK1ε in particular, are also main targets of roscovitine and CR8 (23). Because all effects of roscovitine/CR8 in PKD have been attributed so far to an inhibition of CDKs, we were interested to find out whether polycystic kidney CK1s could be involved as targets of roscovitine/CR8 and whether CK1 deregulation could be observed in PKD.

Here, we show that CK1s indeed represent targets of roscovitine and CR8 in human and mouse polycystic kidneys. CK1ε is systematically overexpressed (at mRNA and protein levels) in polycystic human and murine kidneys compared with healthy kidneys, regardless of the underlying genetic mutation. Additionally, the CK1α isoform pattern is shifted, and the catalytic activities of both CK1ε and CK1α are increased in polycystic kidneys. Thus, inhibition of CK1ε and CK1α could contribute to the long-lasting attenuating effects of roscovitine and CR8 on cystogenesis. CDKs and CK1s thus might constitute a dual therapeutic target to develop kinase inhibitory PKD drug candidates.

MATERIALS AND METHODS

All animal handling and experimentations were carried out following protocols approved by all Institutional Animal Care and Use Committees at the San Raffaelle Scientific Institute (IACUC-736; ultimately approved by the Italian Ministry of Health), the University of California Santa Barbara, the local government in Regensberg, Germany, in accordance with German Animal Protection law, INSERM (B 75-14-02), the University of Alabama at Birmingham, the Institut de Recherches Cliniques de Montréal, the Canadian Council on Animal Care, and Sanofi-Genzyme (Framingham, MA).

Buffers

Bead buffer. Bead Buffer (BB) consisted of 50 mM Tris, pH 7.4, 250 mM NaCl, 5 mM EDTA, 5 mM EGTA, 5 mM NaF, 0.1% Nonidet P-40, and 1× Roche complete protease inhibitors was used.

Blocking buffer. Blocking buffer consisted of 1 M ethanolamine, pH 8.0.

Coupling buffer. Coupling buffer consisted of 0.1 M NaHCO$_3$ and 0.2 M NaCl, pH 8.3.

Homogenization buffer. Homogenization buffer consisted of 25 mM MOPS, pH 7.2, 15 mM EGTA, 15 mM MgCl$_2$, 60 mM β-glycerophosphate, 15 mM p-nitrophenylphosphate, 2 mM dithiothreitol (DTT), 1 mM sodium orthovanadate, 1 mM NaF, 1 mM phenylphosphate disodium, and 1× Roche complete protease inhibitors was used.

Washing buffer. Washing buffer consisted of 0.1 M CH$_3$COONa, pH 4.0.

Assay buffer C. Assay *buffer C* consisted of 25 mM MOPS, pH 7.2, 5 mM EGTA, 15 mM MgCl$_2$, 60 mM β-glycerophosphate, 30 mM p-nitrophenylphosphate, 2 mM dithiothreitol, 0.1 mM sodium orthovanadate, and 1 mM phenylphosphate disodium.

All chemicals were from Sigma-Aldrich (St. Quentin Fallavier, France), except for the protease inhibitor cocktail (Roche, Mannheim, Germany).

Antibodies and Reagents

Antibodies against the following proteins were obtained commercially: CDK2 (sc-163, polyclonal, 1:500; Santa Cruz Biotechnology, Dallas, TX), CDK5 J-3 (sc-6247, monoclonal, 1:500; Santa Cruz Biotechnology), CDK9 (C12F7, monoclonal, 1:1,000; Cell Signaling Technology, Danvers, MA), CK1α [2655, polyclonal, 1:1,000 (Cell Signaling Technology) and polyclonal, sc-6477, 2 μg/IP (Santa Cruz Biotechnology], CK1ε (610445, monoclonal, 1:500 or 2 μg/IP; BD Transduction Laboratories, Pont de Claix, France,), p21^{cip1} (sc-397, polyclonal, 1:500; Santa Cruz Biotechnology), and ERK1/2 (polyclonal, 1:4,000; Sigma-Aldrich, M7927). Polyclonal anti-PDXK antibodies were generated as previously reported (3) and used at a 1:500 dilution. Polyclonal anti-GDE antibodies were generously provided by Dr. Tomoichiro Asano (Department of Internal Medicine, University of Tokyo). These antibodies were validated by various ways; cell treatment with siRNA or shRNA of corresponding protein (CDK2, CDK5, CK1α, CK1ε, and p21^{cip1}) results in lower Western blot (WB) signal by antibody, positive WB signal after affinity purification on axin-2 (CK1s), a fragment of axin, a scaffolding protein known to bind CK1 (77), positive WB signal after affinity purification of extracts on roscovitine/CR8 ligand (CDKs, CK1s, PDXK, ERKs, and GDE), which was confirmed by mass spectrometry, WB signal competed out for binding of CK1s and CDKs on CR8 beads by CK1 inhibitors and CDK inhibitors, respectively, antibodies immunoprecipitated kinases catalytically active toward CK1 substrates (CK1α, CK1ε), and increased WB signal when protein is overexpressed (p21^{cip1}, ERK1/2, PDXK).

(R)-roscovitine and (S)-CR8 were synthesized by ManRos Therapeutics, as previously described (65). CK1 pan-inhibitors (IC261 and D4476) and a CK1ε-specific inhibitor (PF4800567) were provided by Sigma-Aldrich and Tocris (Bristol, UK), respectively. Reagents were solubilized at 10 mM in 100% dimethylsulfoxide (DMSO).

Tissues from Animal Models and Human Kidneys

Animal tissues were provided by different contributors (Table 1). They were snap-frozen and stored at −80°C until further use. Normal human kidney (NHK) and ADPKD renal tissues were obtained from the Kidney Institute, University of Kansas Medical Center (D. Wallace).

Kinase Interaction Panel (DiscovRx KinomeScan)

Assays were performed essentially as described previously (17, 23). For most assays, kinase-tagged T7 phage strains were grown in parallel in 24-well blocks in an *E. coli* host derived from the BL21

Table 1. *Murine models used in this study*

Model	Name	Mutation/Deletion	Age/Disease Stage	Provider
Jck	juvenile cystic kidney	Missense mutation on *Nek8* gene, G448V, in the highly conserved RCC1 domain of NEK8.	26–64 days (Fig. 7); 64 days in all other experiments/high level of cystogenesis	N. Bukanov and O. Ibraghimov-Beskrovnay.
Bpk	BALB/c polycystic kidney	Abnormal 3′ coding region of the *bicaudal C homolog 1* gene, *Bicc1*	Postnatal day 21/very advanced disease	T. Weimbs
Pkd1flox/−:Ksp-Cre	Polycystic kidney disease 1 (polycystin 1)	*Pkd1* gene inactivated in kidneys	P7/severe development of cystogenesis (mice die at P13)	A. Boletta
Pkd1 extra 11	Polycystic kidney disease 1 (polycystin 1)	Deletion of a fragment of the *Pkd1* gene. Expresses only extracellular domain of PKD1	15–24 mo	M. Trudel
Pkd1$_{TAG26}$	Polycystic kidney disease 1 (polycystin 1)	Mutation on *Pkd1* gene in renal and extra renal tissues	5–7 mo	M. Trudel
Pkd1-cKO	Polycystic kidney disease 1 (polycystin 1)	Conditional knockout of *Pkd1* gene	52–54 days/moderate level of cystogenesis	N. Bukanov and O. Ibraghimov-Beskrovnaya
Pcy	Polycystic	Missense mutation (T1841G) in the mouse ortholog of the human *Nphp3* gene (encoding Nephrocystin-3)	30 wk/mild level of cystogenesis	N. Bukanov and O. Ibraghimov-Beskrovnaya
Pkd2-cKO	Polycystic kidney disease 2 (polycystin 2)	Pkd2 gene inactivation in reneal collecting ducts	4 wk/severe cystogenesis	M. Grosch and R. Witzgall
Cpk	Congenital polycystic kidney	Mutation in the *Cys1* gene	10 or 21 days	M. Mrug
HNF1β	Hepatocyte nuclear factor 1β	Knockout of *Hnf1β* gene in kidneys	21–28 days/mild to severe cystogenesis	E. Fischer and M. Pontoglio
Thm1-cKO	Tetratricopeptide repeat-containing hedgehog modulator-1	Conditional knockout of *Thm1* gene (ROSA26-Cre^{ERT})	Gene deletion at P0/analysis at P42	P. V. Tran
Nphp4	Nephronophthisis 4	Knockout of *Nphp4* gene	4 or 8 mo/no cysts	S. Saunier

strain. *E. coli* were grown to log phase and infected with T7 phage from a frozen stock (multiplicity of infection ~0.1) and incubated with shaking at 32°C until they were lysed (~90 min). The lysates were centrifuged (6,000 *g*) and filtered (0.2 μm) to remove cell debris. The remaining kinases were produced in human embryonic kidney-293 cells and subsequently tagged with DNA for quantitative PCR detection. Streptavidin-coated magnetic beads were treated with biotinylated small molecule ligands for 30 min at room temperature (RT) to generate affinity resins for kinase assays. The liganded beads were blocked with excess biotin and washed with blocking buffer (Sea-Block (Pierce), 1% BSA, 0.05% Tween 20, 1 mM DTT) to remove unbound ligand and to reduce nonspecific phage binding. Binding reactions were assembled by combining kinases, liganded affinity beads, and test compounds in 1× binding buffer (20% SeaBlock, 0.17× PBS, 0.05% Tween 20, 6 mM DTT). An 11-point threefold serial dilution of each test compound was prepared in 100% DMSO at a 100× final test concentration that was subsequently diluted to 1× in the assay. All reactions were performed in polystyrene 96-well plates in a final volume of 0.135 ml. The assay plates were incubated at RT with shaking for 1 h, and the affinity beads were washed four times with wash buffer (1× PBS, 0.05% Tween 20). The beads were then resuspended in elution buffer (1× PBS, 0.05% Tween 20, 0.5 μM nonbiotinylated affinity ligand) and incubated at RT with shaking for 30 min. The kinase concentration in eluates was measured by quantitative PCR. K_ds were determined using 11 dose-response curves (top concentration 30 μM, 3-fold dilutions down) that were performed in duplicate. The K_d reported represents the average of the duplicates, and a value of 40,000 nM indicates that no binding was seen at the highest concentration tested (>30 μM).

Affinity Chromatography Purification on Immobilized Roscovitine and CR8

Preparation of roscovitine and CR8-agarose beads. CNBr-activated sepharose 4B (Sigma-Aldrich) was swollen in cold 1 mM HCl for 30 min. Beads were then activated with coupling buffer containing roscovitine plus linker solution or CR8 plus linker solution at 20 mM. Roscovitine or CR8 with a linker were synthesized as described (3, 23) and coupled overnight, protected from light, under constant rotation at room temperature (RT). After removal of the supernatant, beads were washed with coupling buffer and residual active sites quenched using blocking buffer for 2 h under constant rotation at RT. Beads were washed with washing buffer and BB and brought to a 20% suspension in BB. They were stored at 4°C until further use.

Affinity chromatography of roscovitine and CR8-interacting proteins. Just before use, 100 μl of packed beads was washed with 1 ml of BB and resuspended to a 20% suspension in this buffer. The tissue extract supernatant (700 μg of total protein) was then added, and the volume was adjusted to 1 ml with BB. The tubes were rotated at 4°C for 30 min. After a brief spin at 100 *g* and removal of the supernatant, the beads were washed four times with BB before addition of 45 μl of 1× sample loading buffer (Invitrogen) with 200 mM DTT. Following heat denaturation for 3 min and a 1-min spin at 10,000 g, the bound proteins were analyzed by SDS-PAGE and Western blotting (WB).

Competition experiments. Protein extracts were incubated with unattached (free) molecules (CK1 inhibitors) for 10 min at 4°C under constant rotation before the affinity chromatography step.

Table 2. *PCR primers used in this study*

Gene	Forward Primer	Reverse Primer
CK1ε	5′-tgccatttgaccatcttgg-3′	5′-ttttaaagaaaatgcagtgaagaca-3′
CK1α	5′-aaggactgaaggctgcaacaaag-3′	5′-ccccttacacaacacctcaaca-3′
CK1δ	5′-ggctccttcggagacatcta-3′	5′-tgaggatgtttggttttgaca-3′
CK1γ1	5-'ttcccctccatgttgagcta-3′	5′-taggcgcctgtggacttatt-3′
CK1γ2	5′-gaagccaccaagatgagcac-3′	5′-gctcccggctattgacac-3′
CK1γ3	5′-agattctataagcagttaggatctgga-3′	5′-caaacaaatcctccaaactcg-3′
TBP	5′-aggagccaagagtgaagaacaatc-3′	5′-ccaccatgttctggatcttgaagt-3′

CK1, casein kinase 1; TBP, TATA-binding protein.

Affinity Chromatography Purification of CK1 on Axin Beads

Expression of GST-axin 2 fusion protein. The GST-axin 2 fusion protein (77) was expressed in *E. coli* KRX (Stratagene; Agilent Technologies, Les Ulis, France) after induction with 0.5 mM isopropyl β-D-1-thiogalactopyranoside (IPTG) at 37°C for 3 h. Bacteria were resuspended in 20–30 ml of lysis buffer, 1 mg/ml lysozyme was added, and the mix was rotated for 10 min at RT. Lysis extracts were sonicated for 2 min. Six mM $MgCl_2$ and 25 U/ml benzonase were added and incubation pursued for 15 min at 4°C, followed by a spin at 12,000 g for 30 min at 4°C. Soluble fractions were transferred to glutathione beads, followed by a 1-h incubation at 4°C. The beads were washed with lysis buffer three times and once with BB and brought to a 20% suspension in BB. They were stored until further use at 4°C.

Purification of CK1 from kidney lysates. Kidney lysate (600 μg), prepared as described below, was incubated with 100 μl of GST-axin 2-coupled glutathione beads for 30 min at 4°C under constant rotation. The beads were washed four times with BB before the addition of 90 μl of 2× sample loading buffer (Invitrogen) with 200 mM DTT. Following heat denaturation for 3 min, the bound proteins were analyzed by SDS-PAGE and WB, as described below.

Immunoprecipitation of CK1ε and CK1α

Tissue extracts containing 400 μg of total protein were diluted in homogenization buffer to a volume of 500 μl and precleared with 25 μl of protein G sepharose beads (40% slurry in BB; Sigma-Aldrich) at 4°C for 1 h. CK1ε or CK1α were immunoprecipitated with 2 μg of CK1ε or CK1α antibodies, respectively, from precleared lysates by 1 h of incubation at 4°C, followed by 1 h of incubation at 4°C with 25 μl of protein G sepharose beads. Immunoprecipitates were washed four times with BB before the addition of 45 μl 1× sample loaded buffer with 200 mM DTT. Beads were then denatured for 3 min at 99°C. The supernatant was recovered after a 1-min centrifugation at 10,000 g. Diluted and precleared extracts were diluted to one-half in 2× sample loaded buffer containing 400 mM DTT. Immunoprecipitated proteins were analyzed by SDS-PAGE and WB.

Western Blot Analysis

Tissues were weighed, homogenized, and sonicated in homogenization buffer (5 ml/g of material). Homogenates were centrifuged for 10 min at 21,000 g at 4°C. The supernatant was recovered, assayed for protein content (Bio-Rad DC Protein Assay), and kept at −80°C until use. Proteins were prepared at 2 μg/μl in 1× loading buffer with 200 mM DTT and then denatured at 99°C for 3 min. Proteins (30 μg) were separated by 10% NuPAGE precast Bis-Tris polyacrylamide minigel electrophoresis (Invitrogen) with MOPS-SDS running buffer, followed by immunoblotting analysis. Proteins were transferred to 0.45-μm nitrocellulose filters (Whatman, Buckinghamshire, UK). These were blocked with 5% low fat milk in Tris-buffered saline-Tween 20 and incubated overnight at 4°C with antibodies. Appropri-
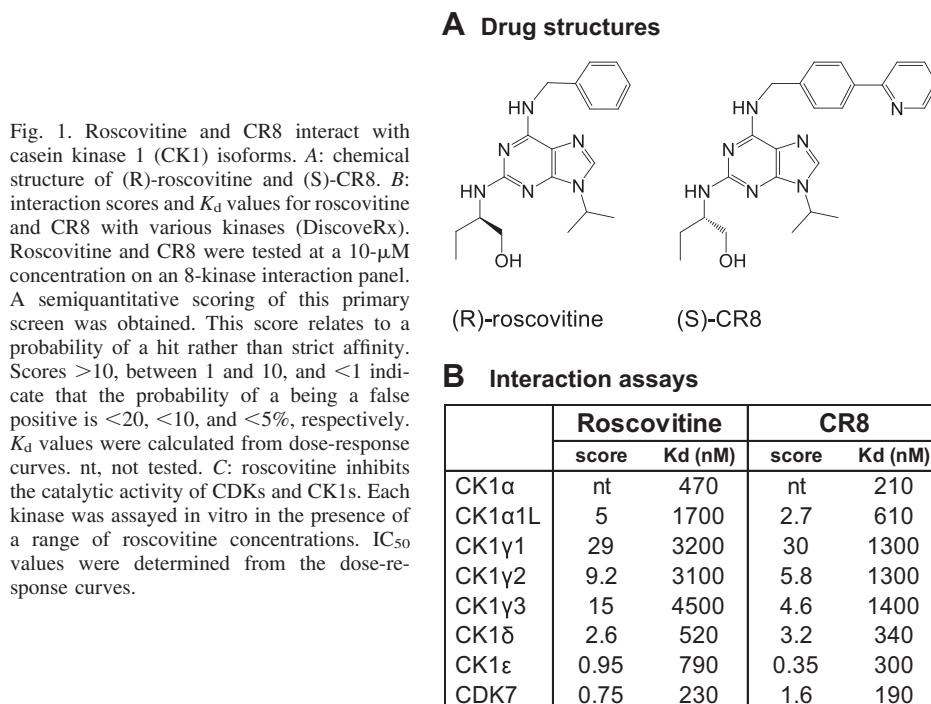

Fig. 1. Roscovitine and CR8 interact with casein kinase 1 (CK1) isoforms. *A*: chemical structure of (R)-roscovitine and (S)-CR8. *B*: interaction scores and K_d values for roscovitine and CR8 with various kinases (DiscoveRx). Roscovitine and CR8 were tested at a 10-μM concentration on an 8-kinase interaction panel. A semiquantitative scoring of this primary screen was obtained. This score relates to a probability of a hit rather than strict affinity. Scores >10, between 1 and 10, and <1 indicate that the probability of a being a false positive is <20, <10, and <5%, respectively. K_d values were calculated from dose-response curves. nt, not tested. *C*: roscovitine inhibits the catalytic activity of CDKs and CK1s. Each kinase was assayed in vitro in the presence of a range of roscovitine concentrations. IC_{50} values were determined from the dose-response curves.

A Drug structures

(R)-roscovitine   (S)-CR8

B Interaction assays

	Roscovitine		CR8	
	score	Kd (nM)	score	Kd (nM)
CK1α	nt	470	nt	210
CK1α1L	5	1700	2.7	610
CK1γ1	29	3200	30	1300
CK1γ2	9.2	3100	5.8	1300
CK1γ3	15	4500	4.6	1400
CK1δ	2.6	520	3.2	340
CK1ε	0.95	790	0.35	300
CDK7	0.75	230	1.6	190

C Kinase assays

Kinase	IC50 (μM)
CDK1/cyclin B1	8.1
CDK2/cyclin E1	0.22
CDK5/p25	0.95
CDK5/p35	0.31
CDK7/cyclin H/MAT1	1.20
CDK9/cyclin K	1.40
CDK9/cyclin T1	1.10
CDK12/cyclin K	3.60
CDK17/p35	22.00
CDK19/cyclin C	>100
CDK20/cyclin T1	13.00
CK1α1	20.00
CK1γ1	19.00
CK1γ2	5.70
CK1γ3	12.00
CK1δ	1.30
CK1ε	3.30

ate secondary antibodies conjugated to horseradish peroxidase (Bio-Rad) were added to visualize the proteins using the enhanced chemi-luminescence reaction.

Protein Kinase Assays

CK1ε or CK1α was immunoprecipitated as described above. After three washes, beads and immobilized immunoprecipitates were washed two times in *buffer C*. The catalytic activity of CK1 bound to beads was assayed in *buffer C* with 50 µM CK-S peptide (RRKHAAIGpSAYSITA; phosphorylated serine (pS); Proteogenix, Schiltigheim, Germany) in the presence of 15 µM cold ATP (Sigma-Aldrich) + [γ-^{33}P] ATP (3,000 Ci/mmol; 10 mCi/ml) in a final volume of 30 µl. The reaction was started by addition of the substrate and ATP mix. Tubes were incubated at 30°C for 30 min. During incubation, tubes were shortly vortexed every 2 min. At the end of the incubation, tubes were briefly centrifuged at 9,600 *g*, and the reaction was stopped by spotting 25 µl of the reaction mix onto P81 phospho-cellulose Whatman filters (Merck Millipore, Darmstadt, Germany), which were washed five times in 1% phosphoric acid. Their radioactivity was measured by a scintillation counter Tri-Carb 2800TR (Perkin-Elmer, Waltham, MA) in the presence of 1 ml of scintillation fluid (Ultima Gold XR; Perkin-Elmer). Kinase activities were expressed in counts per minute incorporated for 30 min.

Kinase Selectivity Panel

The IC$_{50}$ profile of roscovitine and CR8 was determined in a biochemical activity assay using 17 protein kinases by ProQinase (D-79106; Freiburg, Germany). IC$_{50}$ values were measured by testing 10 semi-log concentrations of the compounds in singlicate in each kinase assay ranging from 3 nM to 100 µM. The final DMSO concentration in the reaction cocktails was 1% in all cases.

A radiometric protein kinase assay (33PanQinase Activity Assay) was used for measuring the kinase activity of the 17 protein kinases. All kinase assays were performed in 96-well FlashPlates from Perkin-Elmer (Boston, MA) in a 50-µl reaction volume. The assay for all protein kinases contained 70 mM HEPES-NaOH, pH 7.5, 3 mM MgCl$_2$, 3 mM MnCl$_2$, 3 µM Na-orthovanadate, 1.2 mM DTT, ATP (variable amounts, corresponding to the apparent ATP-Km of the respective kinase), γ-^{33}P-ATP, protein kinase, and substrate.

All protein kinases provided by ProQinase were expressed in Sf9 insect cells or in *E. coli* as recombinant GST fusion proteins or His-tagged proteins either as full-length or enzymatically active frag-
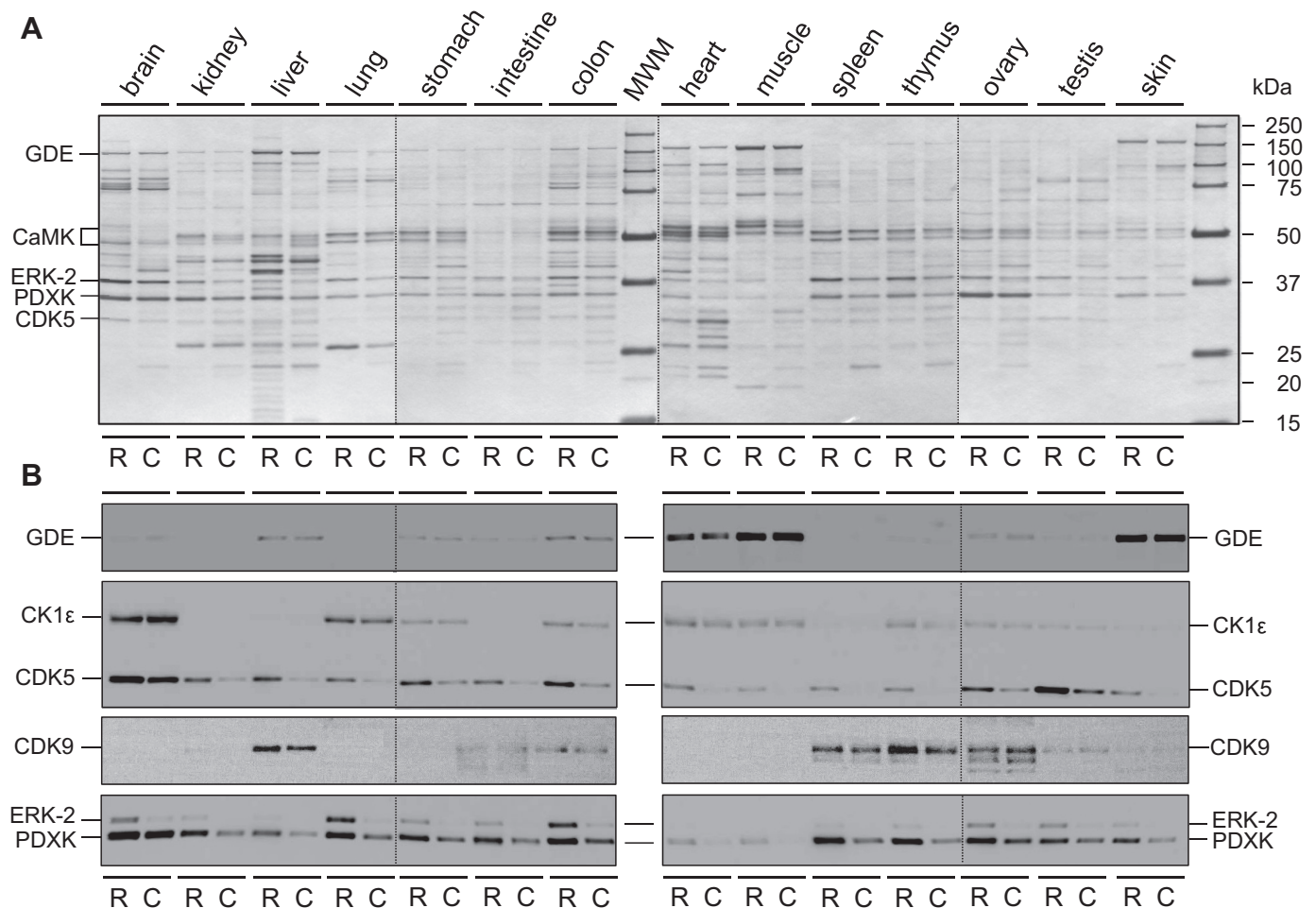

Fig. 2. Affinity chromatography purification of roscovitine and CR8 targets from various mouse tissues. Extracts of healthy tissues (brain, kidney, liver, lung, stomach, intestine, colon, heart, muscle, spleen, thymus, ovary, testis, and skin) were prepared and loaded on immobilized roscovitine (R) and CR8 (C). Beads were extensively washed and the bound proteins resolved by SDS-PAGE (4 different 12-well gels), followed by silver staining (*A*) and Western blotting (WB; *B*), using antibodies directed against glucose-debranching enzyme (GDE), casein kinase 1ε (CK1ε), cyclin-dependent kinase (CDK)5 and CDK9, extracellular-regulated kinase 2 (ERK2), and pyridoxal kinase (PDXK). Note the high CK1ε expression in brain compared with kidney (the latter is not visible due to the short exposure required to avoid oversaturation of the brain CK1ε signal). Vertical dotted lines separate the 4 different gels and 4 different WB assembled in *A* and *B*.

ments. All kinases were produced from human cDNAs. Kinases were purified by either GSH-affinity chromatography or immobilized metal affinity chromotography. Affinity tags were removed from a number of kinases during purification. The purity of the protein kinases was examined by SDS-PAGE/Coomassie staining, and the identity was checked by mass spectroscopy. CK1 isoforms were obtained from Life Technologies (Invitrogen).

The reaction cocktails were incubated at 30°C for 60 min. The reaction was stopped with 50 µl of 2% (vol/vol) H_3PO_4, and plates were aspirated and washed two times with 200 µl 0.9% (wt/vol) NaCl. Kinase activity-dependent transfer of ^{33}Pi (counting of "counts/min") was determined with a microplate scintillation counter (Microbeta; Wallac). All assays were performed with a BeckmanCoulter Biomek 2000/SL robotic system.

RNA Isolation and Real-Time RT-PCR

Total RNA was isolated from tissue using the RNeasy Plus kit (Qiagen, Hilden, Germany) according to the manufacturer's protocol. Total RNA (1 µg) was reverse transcribed by the SuperScript VILO cDNA synthesis kit (Invitrogen, Cergy Pontoise, France) in accordance with the manufacturer's instructions. RNA expression profiles were analyzed by real-time quantitative PCR using SsoFast EvaGreen Supermix (Bio-Rad, Hercules, CA) in a CFX96 Touch real-time PCR detection system (Bio-Rad). Primers used for the detection of *Ck1ε*, *Ck1α*, *Ck1δ*, *Ck1γ1*, *Ck1γ2*, and *Ck1γ3* genes and housekeeping gene *Tbp* are listed in Table 2 (Eurofins, Ebersberg, Germany). The complete reactions were subjected to the following program of thermal cycling: 1 cycle of 30 s at 95°C and 50 cycles of 5 s at 95°C and 5 s at 60°C. A melting curve was run after the PCR cycles, followed by a cooling step. Each sample was run in duplicate in each experiment. Expression levels of *Ck1ε*, *Ck1α*, *Ck1δ*, *Ck1γ1*, *Ck1γ2*, and *Ck1γ3* were normalized to the expression level of *Tbp*.

Histopathology and Image Analysis

Kidneys, cut through the middle, were fixed in 4% buffered formaldehyde and dehydrated and embedded in paraffin wax at 56°C with Excelsior (Thermofisher). Paraffin-embedded samples were cut into sections of 5-µm thickness and stained by hematoxylin and eosin. Three sections separated by 50 µm were analyzed for each kidney. The histological slides were converted to digital slides with a digital slide scanner (Hamamatsu NDP) and analyzed with NIS-Elements software (Nikon). After calibration, kidney and cyst segmentation was performed by thresholding, and the same threshold was performed for all slices. Regions of interest were defined by manual delineation of borders. Total cyst area and cyst number were quantified to calculate the mean cyst area per kidney section.

Statistical Analysis

Statistical analysis was evaluated using Student's *t*-test (computed using GraphPad Prism 5 software). A *P* value = 0.01 to 0.05 was considered significant, a *P* value = 0.001 to 0.01 was considered very significant, and a *P* value of <0.001 was considered extremely significant.

RESULTS

CK1s as Targets of Roscovitine and CR8 in Kidneys

The DiscoveRx KinomeScan interaction assay (17), which includes 402 kinases, revealed the interaction of roscovitine and CR8 (Fig. 1*A*) with CK1 isoforms (23). K_d determinations showed specificity for CK1α, CK1δ, and CK1ε (Fig. 1*B*). The effects of roscovitine on a range of CDKs and CK1s were evaluated in vitro and IC$_{50}$ values determined from dose-
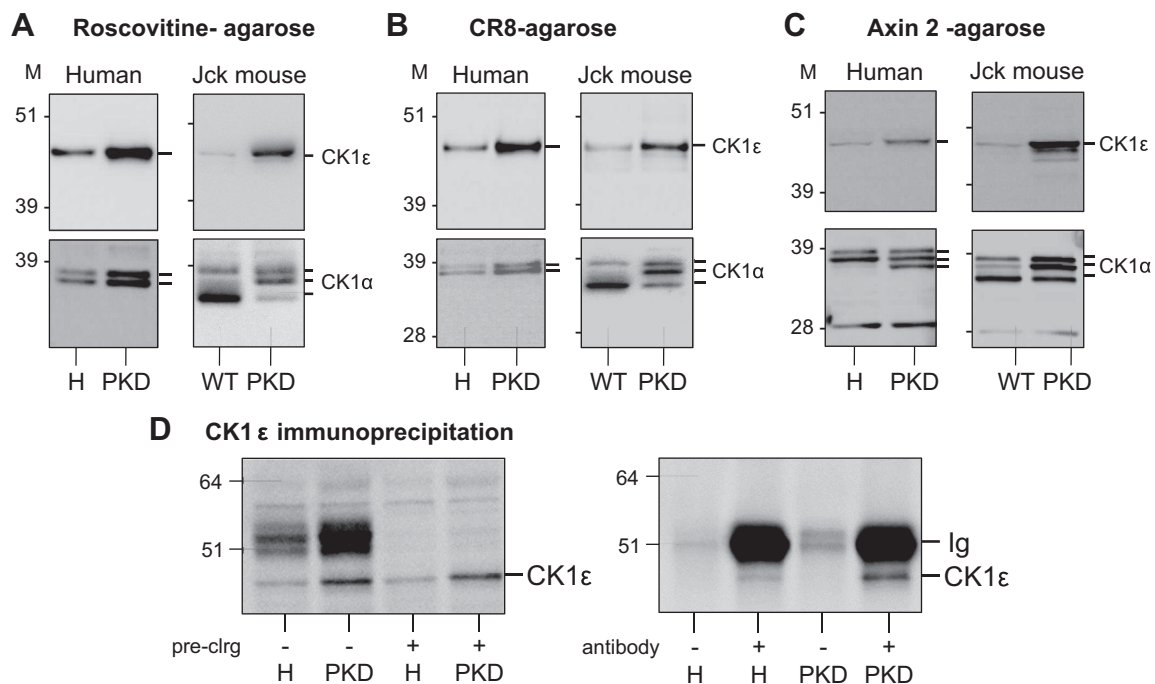

Fig. 3. CK1ε is overexpressed in polycystic kidneys. Roscovitine and CR8-binding proteins in healthy and polycystic kidneys. *A–C*: equal amounts of extracts, prepared from human (*left*) and *jck* mouse (*right*) healthy (H) and polycystic [polycystic kidney disease (PKD)] kidneys, were loaded on roscovitine (*A*), CR8 (*B*), or axin 2 (*C*) beads. After extensive washing, the bound proteins were resolved by SDS-PAGE followed by WB with antibodies directed against CK1ε or CK1α. M, molecular weight markers. *D*: increased CK1ε in PKD vs. healthy kidneys is also seen following immunoprecipitation. *Left*: extracts of H and PKD kidneys (*jck*) were first precleared or not on protein G agarose, and total proteins were resolved by SDS-PAGE followed by WB with anti-CK1ε. Note the increased expression of CK1ε maintained following preclearing. *Right*: CK1ε was next immunoprecipitated from precleared H and PKD kidney extracts and detected by WB. Note the absence of CK1ε in the absence of antibodies and the increased expression of immunopurified CK1ε in PKD vs. H kidneys.
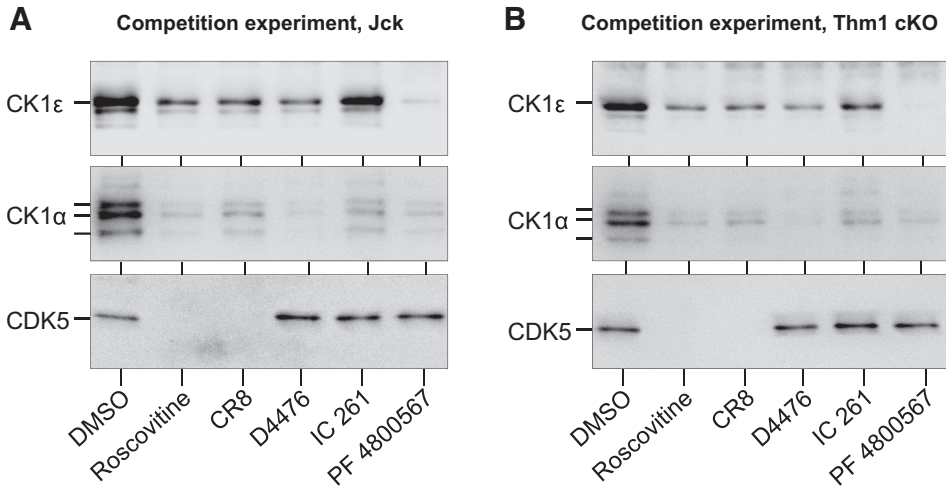
A Competition experiment, Jck

B Competition experiment, Thm1 cKO

Fig. 4. Competition experiments. PKD kidneys from *jck* (*A*) and *Thm1*-conditional knockout (cKO) (*B*) mice were loaded on CR8-agarose beads in the presence of vehicle (DMSO), 250 μM roscovitine or CR8 (both interact with CK1 and CDK5), or 50 μM D4476, IC261 (general CK1 inhibitors), or PF 4800567 (CK1ε specific inhibitor) (the latter 3 do not interact with CDK5). After extensive washing, the bound proteins were analyzed by SDS-PAGE and WB, with antibodies directed against CK1ε, CK1α and CDK5. Note that all products reduce the binding of CK1ε and CK1α, whereas only roscovitine and CR8 compete for CDK5 binding.

response curves (Fig. 1*C*), showing a preference of roscovitine for CDK2, CDK5, CDK7, CDK9, CK1δ, and CK1ε.

Affinity Purification of Kidney Drug Targets on Immobilized Roscovitine and CR8

To identify the targets of roscovitine and CR8 in healthy and polycystic kidneys, we used an affinity chromatography method exploited previously with various CDK inhibitors (3, 47). Compounds were immobilized through a linker on agarose beads. Extracts of healthy mouse tissues were loaded on immobilized roscovitine or CR8, the beads were washed extensively, and the bound proteins were resolved by SDS-PAGE, followed by silver staining and Western blotting (Fig. 2). Results show a panel of targets that vary strikingly in terms of identity and/or quantity according to tissue type (Fig. 2).

We next investigated roscovitine and CR8 targets in kidneys using healthy and polycystic renal tissue. The latter derived from ADPKD patients and from *jck* (C57BL/6J) mutant mice (9 wk old). Kidney extracts were prepared and analyzed by

SDS-PAGE/silver staining. Despite gross morphological differences between healthy and polycystic kidneys, the global protein pattern remained quite similar in the absence or presence of cysts (data not shown).

Kidney extracts were next loaded onto immobilized roscovitine or CR8, beads were washed extensively, and bound proteins were resolved by SDS-PAGE, followed by silver staining (data not shown) and WB using antibodies against CDK2, -5, -7, and -9, glucose-debranching enzyme (GDE), CK1ε, CK1α, ERK1/2, and pyridoxal kinase (PDXK) (data not shown). Extracts were also loaded onto axin-1 and axin-2 agarose beads, which bind glycogen synthase kinase 3 (GSK-3) (74) and CK1s (77), respectively. No major differences were observed between healthy and polycystic kidneys at the level of silver stained proteins. The healthy and polycystic kidney proteins bound to either roscovitine or CR8 were found to be quite similar at the WB level. Only modest differences were observed between the healthy and pathological states in levels of CDK2, CDK5, and CDK7, whereas CDK9 was consistently
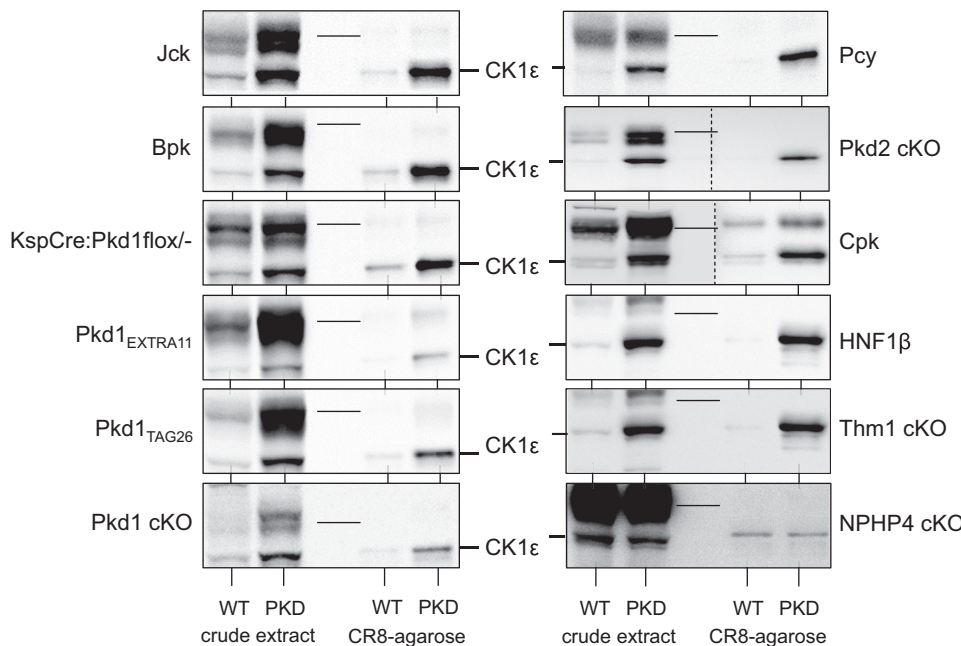

Fig. 5. CK1ε is overexpressed in multiple PKD models. Extracts were prepared from kidneys of mouse PKD and corresponding WT animals and analyzed directly (crude extract) or following affinity purification on CR8-agarose beads. SDS-PAGE was followed by WB with antibodies directed against CK1ε. The non-polycystic nephronophthisis (*Nphp 4*) model, used as a control, displayed no change in CK1ε expression. Thin lines in the blots indicate the position of the 51-kDa molecular weight marker (MWM). Crude extracts and CR8-purified proteins, separated by a MWM lane, were run on the same gel, and a single WB blot was carried out for all 4 samples for each mouse model. In Cpk samples, because of important signal intensity differences, different exposures were necessary for crude extracts and CR8-purified proteins. The 2 WB, assembled in a single panel, are thus separated by a vertical dotted line. In Pkd2-cKO samples, crude extracts and CR8-agarose were not separated by MWM, and the WB was cut and separated by a blank space delineated by a vertical dotted line.

Fig. 6. The CK1α isoform pattern is modified similarly in all PKD models. Extracts were prepared from kidneys of mouse PKD and corresponding WT animals and analyzed directly (crude extract) or following affinity purification on CR8-agarose beads. SDS-PAGE was followed by WB with antibodies directed against CK1α. The nonpolycystic nephronophthisis model, used as a control, displayed no change in CK1α expression or isoforms pattern. Thin lines in the blots indicate the position of the 39-kDa MWM. Crude extracts and CR8-purified proteins, separated by a MWM lane, were run on the same gel, and a single WB blot was carried out for all 4 samples for each mouse model. In Thm1-cKO samples, because of important signal intensity differences, different exposures were necessary for crude extracts and CR8-purified proteins. The 2 WBs, assembled in a single panel, are thus separated by a vertical dotted line. In Pkd2-cKO samples, crude extracts and CR8-agarose were not separated by MWM, and the WB was cut and separated by a blank space delineated by a vertical dotted line.
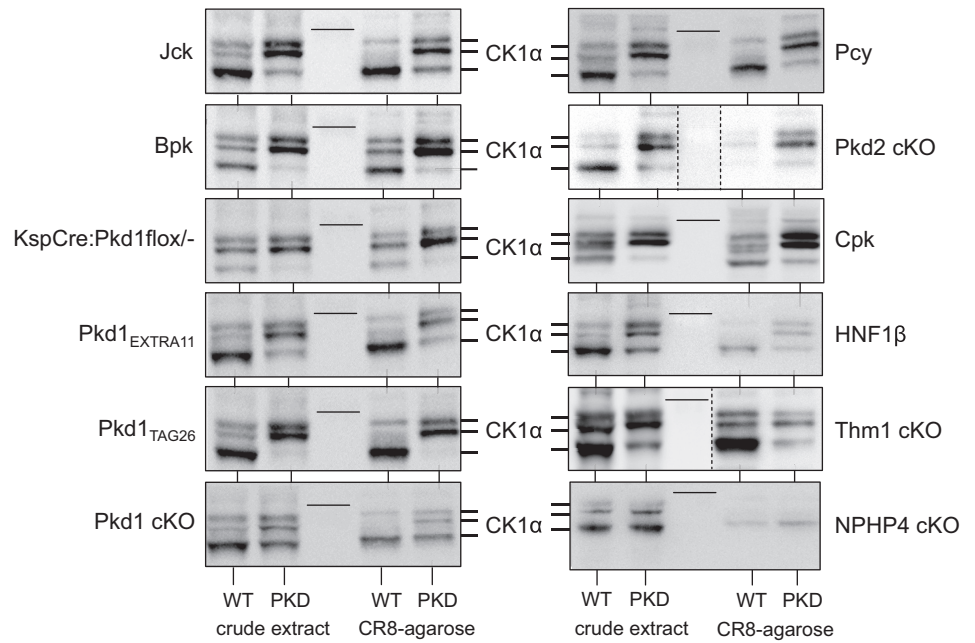
increased in polycystic extracts. No differences in GDE, ERK1/2, PDXK, or GSK-3 were seen (data not shown).

CK1ε Is Overexpressed While the CK1α Isoforms Pattern Is Altered in Polycystic Kidneys

In contrast, the level of CK1ε was consistently increased in both human and mouse polycystic kidneys, whereas the electrophoretic pattern of CK1α was consistently modified (decrease of the lower band, increase of middle and upper bands), as seen after affinity purification on roscovitine-agarose, CR8-agarose, and axin-2 -agarose (Fig. 3, A–C). Binding specificity was demonstrated in competition experiments with various inhibitors (Fig. 4). CK1ε was next immunoprecipitated (with/

without protein A-agarose preclearing) from healthy and *jck* polycystic kidneys by a specific antibody. WB analysis revealed strong CK1ε induction (Fig. 3D). The same experiment was performed with anti-CK1α antibodies. Preclearing maintained the change in CK1α pattern seen in polycystic vs. healthy kidneys (data not shown). Only the upper form of CK1α was immunoprecipitated (data not shown).

To determine whether aberrant expression pattern of CK1ε and CK1α is a general characteristic of cystic kidneys regardless of the genetic mutation, we investigated the expression of CK1ε and CK1α in a variety of PKD mouse models (Figs. 5 and 6). Extracts of cystic and unaffected kidneys from the corresponding mouse strain were prepared and analyzed by

Fig. 7. Expression of CDK2 and p21^{cip1} in the kidneys of a variety of mouse PKD models. Extracts were prepared from kidneys of mouse PKD and corresponding WT animals and analyzed directly (crude extract) or following affinity purification on CR8-agarose beads. SDS-PAGE was followed by WB with antibodies directed against CDK2 and p21^{cip1}. The nonpolycystic nephronophthisis model, used as a control, displayed no change in CDK2 expression but an increase in p21^{cip1}. Thin horizontal lines on the *left* of the CDK2 and p21^{cip1} blots indicate the position of the 39- and 21-kDa MWM, respectively. Thin lines on the *right* of the blots indicate the positions of CDK2 and p21^{cip1}, respectively.
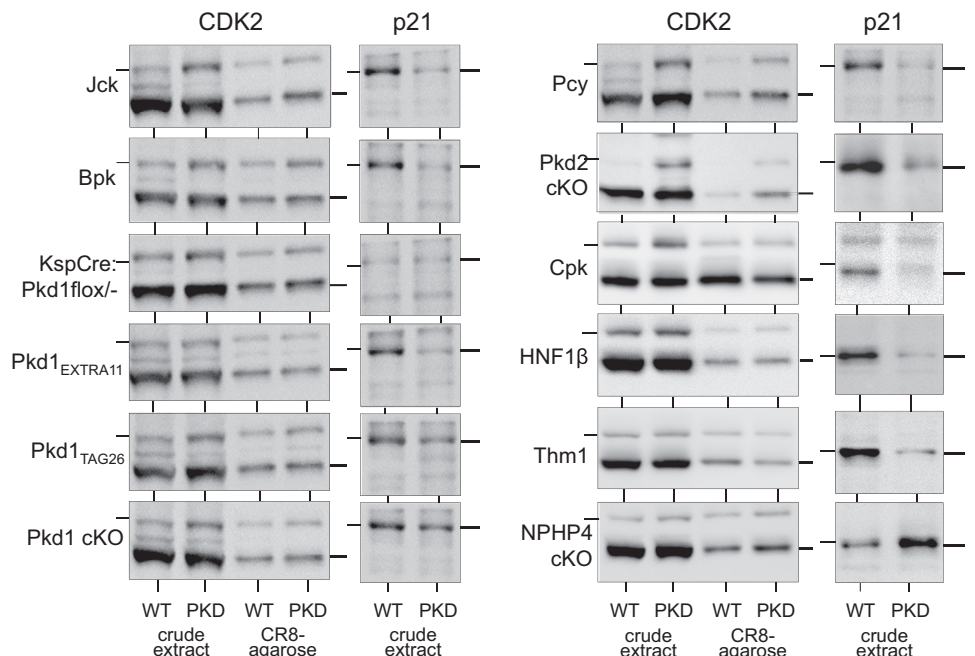
WB as crude extracts or following purification on CR8-agarose. CK1ε was overexpressed (Fig. 5), whereas the CK1α isoforms pattern was modified (Fig. 6) in a similar fashion in all PKD models. In contrast, no changes in CK1ε expression or in CK1α isoform patterns were observed in the *Nphp4*-knockout (KO) mouse model of nephronophthisis, which does not develop cysts. In parallel, p21^{cip1} (a natural CDK2 inhibitor), CDK2, CDK5, and CDK9 expression was analyzed in the same crude extracts and/or following CR8-agarose affinity purification. Expression of p21^{cip1} was always reduced in polycystic vs. healthy kidneys, in the mice models used in this study, as described in Pkd1$^{-/-}$ (7) and Kif3a$^{-/-}$ mutant mice (53), (Fig. 7), Han:SPRD rats (67) and human ARPKD renal tissue (see Ref. 67 and Billot K, Coquil C, and Meijer L, unpublished data). In contrast, p21^{cip1} expression was increased in the *NPHP4*-KO kidney extracts. CDK2 expression was very stable in all PKD models (Fig. 7), whereas that of CDK5 was increased in seven of 11 tested PKD models and that of CDK9 almost always increased (data not shown).

CK1ε mRNA Is Overexpressed in Polycystic Versus Healthy Kidneys

The mRNA levels of all CK1 isoforms in the kidneys of *jck* and *Pkd1*-conditional knockout (cKO) mice, and their wild-type (WT) littermates, were quantified by Q-PCR, using TBP (TATA-binding protein) as a house-keeping reference mRNA (Fig. 8, *A* and *B*). CK1ε mRNA was increased in PKD kidneys of both mouse mutants, while mRNA levels of other CK1 remained essentially stable (Fig. 8, *A* and *B*). We also measured the mRNA levels of *CK1ε* and *CK1δ* in the remaining 9 PKD models used in this study (Fig. 8*C*). *CK1ε* mRNA is upregulated, while the mRNA levels of the closely related *CK1δ* remained stable in all PKD models (Fig. 8*C*). In contrast to PKD models, *CK1ε* mRNA expression remained stable in the non-cystic, *Nphp4* model. Altogether these results suggest that PKD development is associated with an increase in CK1ε mRNA and protein expression, while expression of other CK1 isoforms remains constant.
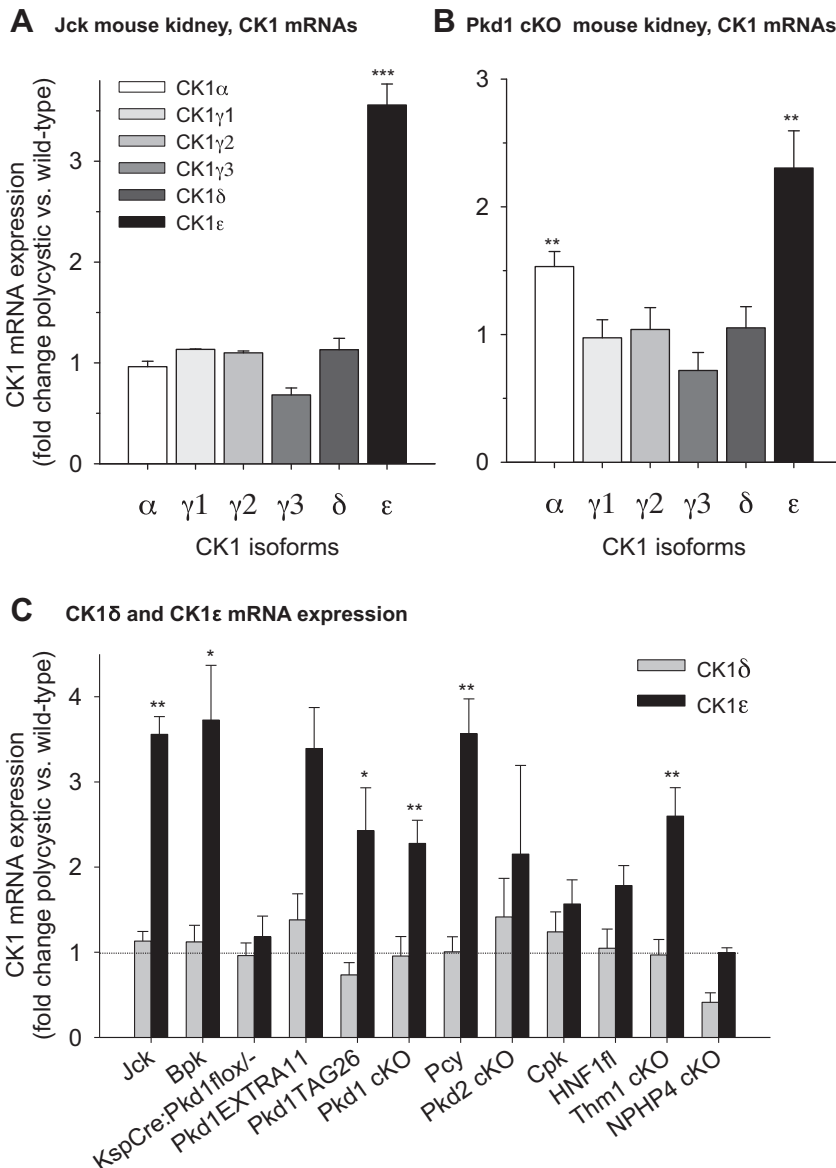

A Jck mouse kidney, CK1 mRNAs

B Pkd1 cKO mouse kidney, CK1 mRNAs

C CK1δ and CK1ε mRNA expression

Fig. 8. CK1ε mRNA expression is increased in representative PKD models. *A*: mRNA expression levels of all CK1 isoforms in kidneys of *jck* and wild-type (WT) mice were quantified by PCR. The values were normalized on the basis of TATA-binding protein (TBP) mRNA levels and are expressed as fold change in polycystic over WT kidney levels. *B*: expression levels of all CK1 isoforms in *Pkd1*-cKO and control mouse kidneys. *C*: expression levels of CK1ε and CK1δ isoforms in the kidneys of various PKD models, normalized with *TBP* mRNA levels and presented as fold change of polycystic over healthy kidneys levels. Horizontal dotted line indicates identical level of expression for healthy and polycystic kidneys. Number of different kidneys (WT/PKD): 2/3 (Jck), 3/3 (Bpk), 2/2 (KspCre), 4/4 (Tag26), 2/2 (Extra 11), 4/4 (Pkd1cKO), 3/3 (Pcy3), 2/2 (Pkd2cKO), 4/4 (Cpk), 4/4 (Hnf1β), 5/4 (Thm1cKO), and 3/3 (Nphp4). Tested in triplicate. *$P = 0.01–0.05$, **$P = 0.001–0.01$, and ***$P < 0.001$ (Student's *t*-test).

Tissue Distribution of CK1ε and CK1α Expression Changes

We analyzed CK1ε and CK1α mRNA levels in various *jck* and *Pkd1*-cKO mice tissues, relative to levels of wild-type (WT) littermates (Fig. 9, *A* and *B*). CK1ε mRNA was overexpressed in polycystic kidneys but not in other tissues. In healthy mice the CK1ε protein is expressed mostly in brain, lung, and heart (Fig. 2). We analyzed protein levels of CK1ε, CK1α, and p21^{cip1} in kidneys, liver, heart, and brain of *jck* and *Pkd1*-cKO mice and healthy WT animals (Fig. 9, *C* and *D*). An increase in CK1ε expression, a change in CK1α isoform pattern and a decrease in p21^{cip1} expression were seen in the kidneys of both polycystic models compared with WT littermates, but these changes were not present in liver, heart, or brain (Fig. 9C). In polycystic animals, CK1ε and CK1α expression changes are thus limited to the kidneys. It is surprising that no changes were seen in the liver (Fig. 9C), since polycystic liver is frequently observed associated with PKD. Nevertheless, this lack of expression changes correlates well with the very modest increases in liver CK1ε and CK1α catalytic activities (Fig. 10, *C* and *D*). Differences in timing of expression/activity changes between kidney and liver may explain these differences.

### Time Course of CK1ε and CK1α Expression Changes

A time course of CK1 expression changes during disease progression was charted in *jck* mouse kidneys collected from 26 to 64 days after birth (Fig. 10). Histological analysis and quantification of cyst surface area illustrate the development of cysts over time (Fig. 10, *A* and *B*). *CK1ε* mRNA levels were already upregulated at the very first time point and continuously increased in parallel with increased cystic volume (Fig. 10C). In contrast *CK1α* mRNA levels remained constant throughout the time course (Fig. 10D). WB analysis of CR8-agarose purified proteins showed that CK1ε protein expression is already increased 26 days after birth (first time point), whereas the CK1α isoform pattern appears to shift progressively with time (Fig. 10E).

CK1ε and CK1α Catalytic Activities Are Increased in Polycystic Kidney Disease

We next analyzed the catalytic activity of CK1ε and CK1α in polycystic and healthy kidneys (Fig. 11). CK1ε and CK1α were immunopurified with specific antibodies from kidneys of *jck*, Pkd1-cKO, *Thm1*-cKO, and *Nphp4*-KO mice and their WT littermates. Kinase activities were assayed using ^{33}P-ATP and CK-S peptide as substrates. Results show increased catalytic activities for both CK1ε (Fig. 11A) and CK1α (Fig. 11B) in the kidneys of the three PKD models, but not of the nephronophthisis model. Note that the basal activity of CK1ε was 25- to 50-fold lower than that of CK1α. Next, kinase activity assays were run following CK1ε and CK1α immunopurification from different tissues of polycystic *Pkd1*-cKO mice (Fig. 11, *C* and *D*). Results

Fig. 9. Alteration in CK1ε and CK1α expression in kidneys of PKD models. *A* and *B*: *CK1ε* and *CK1α* mRNA levels were quantified in kidneys, liver, heart, and brain of *jck* (*A*) and Pkd1-cKO (*B*) mice. PCR data were normalized to TBP mRNA levels and are presented as fold change of polycystic over WT tissue levels. *C* and *D*: CK1ε and CK1α protein levels were estimated by WB in kidneys, liver, heart, and brain of *jck* (*C*) and *Pkd1* cKO (*D*) mice. Equal amounts of crude extracts of WT and PKD mouse tissues were loaded and resolved on SDS-PAGE, and proteins were detected by WB with specific antibodies. GAPDH was used as a loading control. Increased expression of CK1ε and altered CK1α pattern were seen only in the polycystic kidneys compared with WT kidneys. The decrease in p21^{cip1} was confirmed in the kidneys of both models; $n = 1$ for each organ. Tested in triplicate. *$P = 0.01-0.05$, **$P = 0.001-0.01$, and ***$P < 0.001$ (Student's *t*-test).
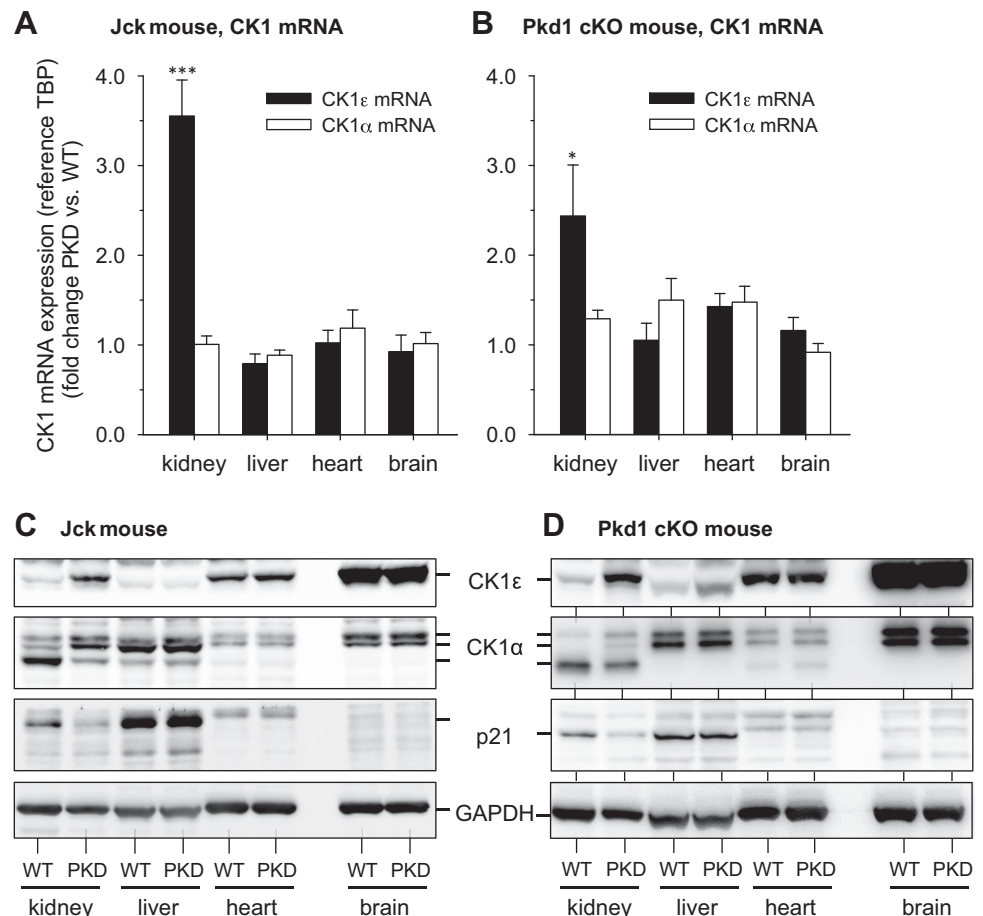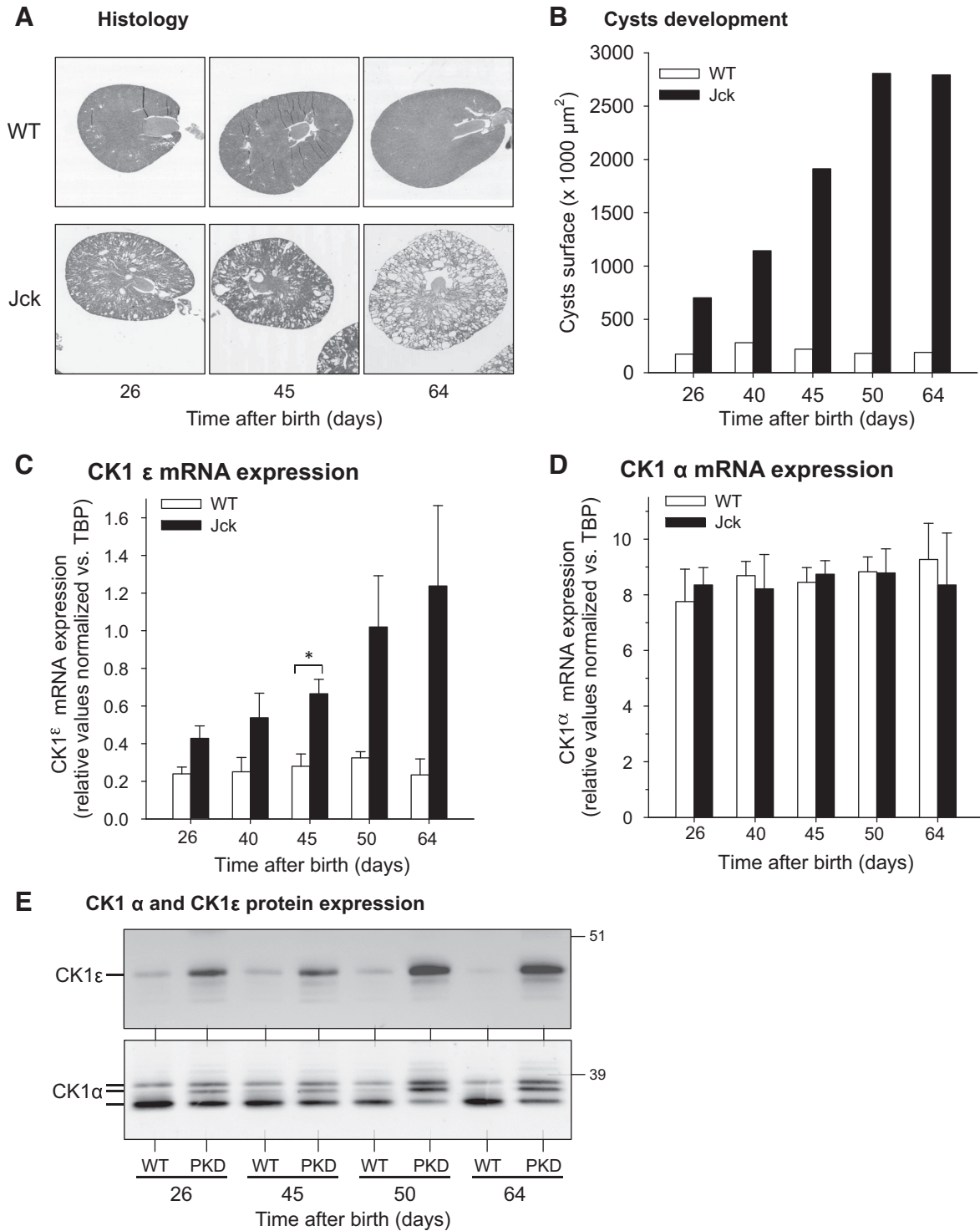
Fig. 10. CK1ε and CK1α expression is altered with PKD progression in *jck* mice. *A*: histology of *jck* and WT kidneys at different times after birth. *B*: quantification of cyst development in *jck* mice. *C* and *D*: *CK1ε* (*C*) and *CK1α* (*D*) mRNA expression levels in *jck* and WT mice kidneys (normalized to TBP levels) at different time points. Number of different kidneys (WT/PKD): $n = 2$ for each time point. Tested in triplicate. *E*: CK1ε and CK1α protein expression in *jck* and WT mice kidneys at different time points. Kidney extracts were loaded on CR8-agarose beads, bound proteins were resolved by SDS-PAGE, and CK1 isoforms were detected by WB with specific antibodies. *$P = 0.01$–0.05 (Student's *t*-test).

show that only kidneys displayed enhanced CK1ε and CK1α activity (Fig.11, *C* and *D*), confirming the renal specificity of CK1ε and CK1α altered expression. Because the antibodies directed against CK1α only immunoprecipitated the upper form (data not shown), we can say only that the catalytic activity of this CK1α isoform is increased in polycystic kidneys. We have no access to the catalytic activity of the two lower forms of CK1α.

Fig. 11. Catalytic activities of CK1ε and CK1α are increased in polycystic kidneys. CK1ε (*A*) and CK1α (*B*) were immunopurified with specific antibodies from kidneys of *jck*, *Pkd1*-cKO, *Thm1*-cKO, and *Nphp4* mutant mice and their control WT littermates. Catalytic activities were assayed using ^{33}P-ATP and a peptide substrate. Activities are reported as ^{33}P-phosphate incorporated/30 min incubation. Number of different assays (CK1ε/CK1α): 2/2 (Jck), 5/3 (Pkd1cKO), 2/2 (Thm1cKO), and 3/3 (Nphp4). Tested in triplicate. CK1ε (*C*) and CK1α (*D*) were immunopurified with specific antibodies from kidneys, liver, heart, and brain of Pkd1-cKO and control mice. Their catalytic activities were assayed with ^{33}P-ATP and a peptide substrate. Activities are reported as ^{33}P-phosphate incorporated/30 min incubation. Numbers inside parentheses represent the kinase activity fold change in recombinant vs. wild-type and control tissues. Number of different assays (CK1ε/CK1α): 5/3 (kidneys), 3/3 (liver), 3/3 (brain), and 3/3 (heart).
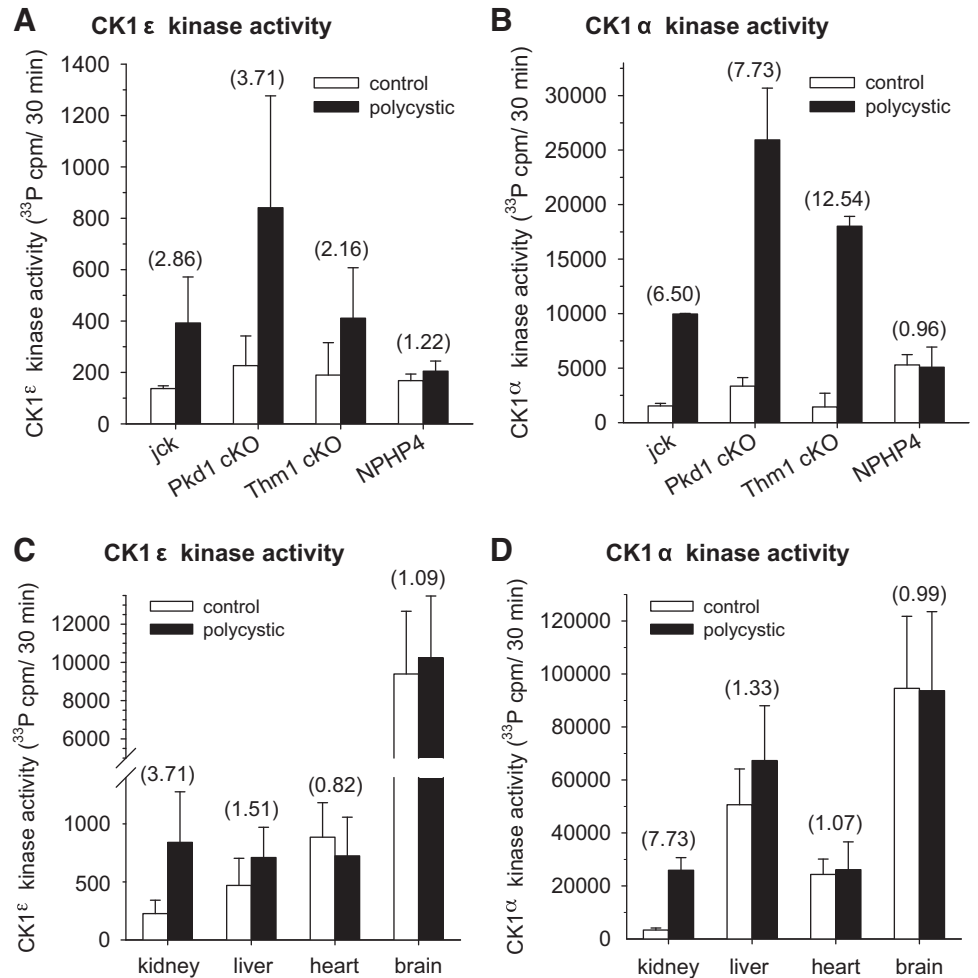
DISCUSSION

CK1 Kinases in Cystogenesis and PKD

This article reports a systematic increase in the catalytic activities of CK1ε and CK1α in polycystic kidneys compared with healthy kidneys. Enhanced kinase activity correlates with increased protein and mRNA expression for CK1ε and a shift in the isoform pattern for CK1α. These modifications of CK1ε and CK1α expressions were observed in 11 PKD mouse models but not in a NPHP4-cKO nephronophthisis model. Enhanced CK1ε protein and mRNA expression levels were also detected in human ADPKD kidneys compared with healthy kidneys (data not shown). We also confirm the inhibition of CK1s by roscovitine and CR8, two kinase inhibitors initially developed against CDKs (5, 6, 19, 58–60), which reduced cystogenesis and preserved renal functions in various animal models of PKD (13, 14, 66, 67, 85). Renal CK1ε and CK1α thus represent additional targets of roscovitine and CR8.

The CK1 family comprises seven members of ubiquitously expressed, highly conserved kinases playing a large diversity of cellular functions (reviewed in Refs. 21 and 46) CK1s have been reported to be involved in Wnt (reviewed in Refs. 21, 22, 24, 41, 46, 75, and 91), Hedgehog (Hh) (reviewed in Refs. 41, 42, and 81), and mTor signaling (reviewed in Refs. 29, 40, 44, 51, and 99), all of which are involved in cystogenesis.

The polycystin complex mediates Wnt signaling (45), a pathway involving both GSK-3 and CK1 (reviewed in Refs. 22 and 41), and axin, a scaffolding protein binding both kinases (75). GSK-3 phosphorylates polycystin 2 at Ser[76], thereby controlling its membrane localization (83). GSK-3 activity has been demonstrated to contribute to cystogenesis (84), and GSK-3 is regulated by a cAMP- and CREB-mediated process (43). CK1 acts as a "priming kinase" for some substrates that then become accessible to phosphorylation by GSK-3 (15). CK1 thus indirectly controls GSK-3 substrates availability.

CK1 phosphorylates several proteins involved in Hh signaling (reviewed in Ref. 41), namely the smoothened (Smo) signal transducer (16, 28, 42) and the fused (Fu) (98) and Gli proteins (Ci/Gli) (71, 81). Through these phosphorylations, CK1 promotes Smo activity, activates Fu, and regulates Ci/Gli processing. Using a kinome RNAi screen, CK1α was identified as a positive regulator of Hh signaling (27). Genetic deletion of *Thm1* (tetratricopeptide repeat-containing hedgehog modulator-1), a negative regulator of Hh signaling, triggers renal cystogenesis. Downregulation of Hh signaling in the *Thm1* cKO mouse by genetic deletion of *Gli2*, a key transcriptional activator of the pathway, reduces cystogenesis (86, 87). Thus we expect CK1 activity to contribute to Hh-dependent cystogenesis and its inhibition to negatively affect PKD development.

Mammalian target of rapamycin (mTOR) is clearly involved in cystogenesis, and despite some controversy, inhibiting mTOR remains a promising therapeutic approach (reviewed in Ref. 29, 40, 44). CK1α is part of an autoamplification loop for mTOR signaling (26). Following a priming phosphorylation by mTOR, the mTOR inhibitor DEPTOR is phosphorylated by CK1α, leading to its proteasomal degradation. Thus mTOR triggers the CK1α-dependent destruction of its inhibitor, leading to enhanced mTOR kinase activity. Downregulation of CK1 activity is thus expected to reduce mTOR signaling.

CK1 is also involved in cell proliferation (reviewed in Ref. 46) For example, CK1ε promotes cell proliferation through 4E-BP1 phosphorylation-dependent regulation of translation (82) and through its action on Wnt signaling (96). Another example is provided by Jade-1S, a protein highly expressed in kidney epithelial cells, which is especially concentrated in primary cilia and centrosomes (12). Jade-1S has several functions associated with injury repair: regulation of Wnt signaling, DNA transcription and epigenetic modifications. CK1α phosphorylation of Jade-1S at Ser^{377} turns off its chromatin remodeling functions, allowing cell cycle progression. Prevention of CK1α-mediated Jade-1S phosphorylation alters the interactome profile of Jade-1S (the mitotic kinase PLK1 and Jade-1S

interact in a CK1α-dependent manner) and is accompanied by impaired cell proliferation (12).

The primary cilium is central to cystogenesis (reviewed in Refs. 2, 10, 36, 39, 54, 55, and 68), and CK1ε was identified in a global proteome study of the primary cilium (61). CK1α was identified in a proteomic study of human airway ciliary axonemes (8). CK1ε (50), CK1α (16), and CK1δ (34) play a role in cilia stability, although many molecular details still need clarification. Taken together, the literature and our results support essential roles of CK1 isoforms in key pathways involved in cilia function and cystogenesis.

CDK/CK1 Dual-Specificity Inhibitors

Various CDKs play a role in cystogenesis in both controlling cell proliferation and regulating cilia functions. The mTOR inhibitor rapamycin downregulates the expression of CDK1 and several cyclins, reduces cyst growth and improves kidney function in a *Pkd2*-cKO model (51). CDK2 expression and activity levels have not been investigated in PKD. However, several reports show that $p21^{cip1}$ expression is decreased in polycystic kidneys (7, 53, 67). We confirmed reduced $p21^{cip1}$ expression in 11 PKD mouse models (Fig. 7) as well as in
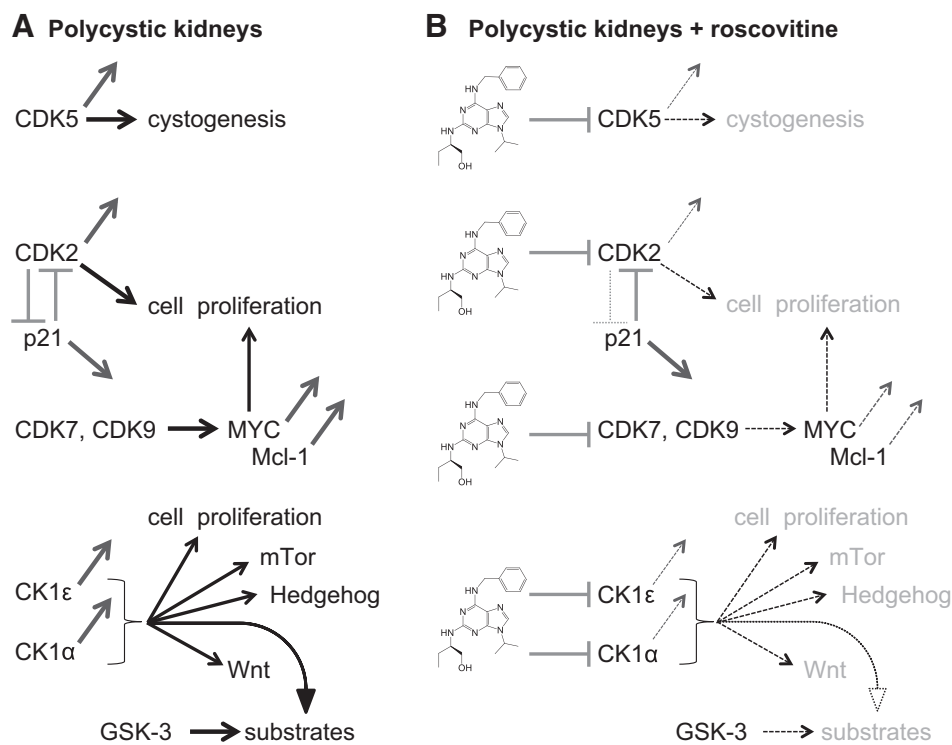

Fig. 12. Roscovitine and CR8 reduce cystogenesis through combined inhibition of CDKs and CK1s, a working hypothesis for the development of a kinase inhibitor drug candidate. *A*: in polycystic kidneys, *1*) CDK5 levels have been reported to be increased, and CDK5 is involved in ciliogenesis and cystogenesis; *2*) $p21^{cip1}$ expression is reduced, leading to enhanced CDK2 activity, and furthermore, CDK2 phosphorylates $p21^{cip1}$ on Ser^{78}, leading to its inactivation; *3*) CDK9 expression is enhanced and may contribute to MYC overexpression in conjunction with CDK7 (both kinases contribute to maintain Mcl-1 expression; decreased $p21^{cip1}$, increased CDK2, and increased MYC all contribute to enhanced proliferation, and elevated Mcl-1 acts to prevent apoptotic cell death; *4*) CK1ε protein level is increased whereas the CK1α isoform pattern is modified, resulting in enhanced kinase activity of both CK1s. CK1s have been reported to be involved in cell proliferation and in mammalian target of rapamycin (mTOR), Hedgehog, and Wnt signaling, all shown to be implicated in cystogenesis. Furthermore, CK1 acts as a "priming kinase" by phosphorylating substrates that then become available for phosphorylation by GSK-3, a kinase also reported to play a key role in cystogenesis. *B*: Reduction of CDK5, CDK2, CDK7, and CDK9 catalytic activities by roscovitine and CR8 is expected to lead to reduced cell proliferation, induction of apoptosis, and reduced cystogenesis. Reduction of CK1ε and CK1α catalytic activities by roscovitine and CR8 is expected to lead to reduced cell proliferation, altered mTOR, Hedgehog, and Wnt signaling, reduced substrate phosphorylation by GSK-3, and ultimately reduced cystogenesis.

kidneys from human patients with ADPKD (data not shown). We can expect CDK2 activity to be increased, despite stable expression, as a consequence of reduced p21[cip1] expression. Furthermore, in a feedback loop, CDK2 inactivates p21[cip1] by phosphorylating its Ser[78] residue (38). Tumor necrosis factor-α (TNFα), present in cyst fluid, downregulates p21[cip1] expression and consequently promotes cyst-lining epithelial cell proliferation (97). A *PKD2* mutant cell line showed reduced expression of p57[Kip2], another natural CDK2 inhibitor, and increased CDK2 levels (30). Interestingly, the ciliary kinase NEK8 participates in the maintenance of genomic stability by reducing CDK2/cyclin A activity. Loss of NEK8 activity (as seen in some ciliopathies, including PKD and nephronophthisis) results in increased CDK activity and DNA damage (18, 33). By inhibiting CDK2 activity directly, CDK inhibitors are thus expected to compensate for the reduction in p21[cip1] levels and, therefore, to prevent cell proliferation. CDK5 expression was reported to be increased in *jck* kidneys (14). We saw upregulation in seven models out of 11 tested (data not shown). Is this differential expression linked to the severity of the disease? CDK5 phosphorylates the centrosomal phosphoprotein NDE1, a negative regulator of cilia length, at Thr[191], targeting NDE1 for ubiquitinylation by the E3 ubiquitin ligase FBW7 and destruction (56). CDK5 or FBW7 depletion stabilizes NDE1 and reduces cilia length (56). Crossing *jck* mice with *CDK5*-cKO mice unambiguously demonstrates that CDK5 activity regulates ciliary length and contributes to cysts formation (30). Inhibition of CDK5 by roscovitine/CR8 may thus contribute to reduce cystogenesis. CDK9 expression was increased in the kidneys of most of the polycystic models we investigated (data not shown). Along with CDK7, CDK9 controls RNA polymerase and thus short-lived proteins. We reported in another context that CDK9/CDK7 inhibition by roscovitine and CR8 leads to reduced expression of Myc (23) and Mcl-1 (5), which contribute to cell proliferation and apoptosis, respectively. Myc overexpression in PKD has been described in detail (reviewed in Ref. 88; also see Refs. 20, 31, and 88–92). Inhibition of CK1ε by chemical inhibitors or shRNA prevented the phosphorylation of 4E-BP1 and reduced c-Myc expression in cell lines (25). We do not know whether roscovitine treatment will lead to a reduction of Myc and Mcl-1 in vivo, which would contribute to reduce cell proliferation and enhance apoptosis. Inhibiting CDKs is further encouraged by recent identification of multiple CDK inhibitors in an in vitro three-dimensional cystogenesis screen (11).

In summary, our results suggest that roscovitine and CR8 may exert their beneficial effects on polycystic kidneys through a dual action (Fig. 12): *1*) inhibition of several CDKs, leading to reduced proliferation and enhanced apoptosis; and *2*) inhibition of CK1ε and CK1α, leading to inhibition of proliferation, altered Wnt, Hh, and mTOR signaling, and indirect inhibition of GSK-3. Development of pharmacological inhibitors with an optimal balance of kinase inhibition between the different CDK and CK1 isoforms is likely to be relevant for controlling PKD progression.

DISCLOSURES

L. Meijer and N. Oumata are coinventors on the CR8 patent. L. Meijer is an inventor on the roscovitine patent. L. Meijer is cofounder, Chair and CSO, of ManRos Therapeutics. The other authors have no conflicts of interest to disclose.

AUTHOR CONTRIBUTIONS

K.B. and L.M. conceived and designed research; K.B., C.C., B.V., B.J.-F., N.D., C.D., N.O., Y.L.M., A.B., T.W., M.G., R.W., S.S., E.F., M.P., A.F., M.M., P.V.T., M.T., N.O.B., and O.I.-B. performed experiments; K.B., C.C., B.V., C.D., D.P.W., and L.M. analyzed data; K.B., C.C., and L.M. interpreted results of experiments; A.B., T.W., M.G., R.W., S.S., E.F., M.P., M.M., D.P.W., P.V.T., M.T., N.O.B., O.I.-B., and L.M. edited and revised manuscript; L.M. prepared figures; L.M. drafted manuscript; L.M. approved final version of manuscript.

REFERENCES

1. **Antignac C, Calvet JP, Germino GG, Grantham JJ, Guay-Woodford LM, Harris PC, Hildebrandt F, Peters DJ, Somlo S, Torres VE, Walz G, Zhou J, Yu AS.** The future of polycystic kidney disease research—as seen by the 12 Kaplan awardees. *J Am Soc Nephrol* 26: 2081–2095, 2015. doi:10.1681/ASN.2014121192.

2. **Avasthi P, Maser RL, Tran PV.** Primary Cilia in Cystic Kidney Disease. *Results Probl Cell Differ* 60: 281–321, 2017. doi:10.1007/978-3-319-51436-9_11.

3. **Bach S, Knockaert M, Reinhardt J, Lozach O, Schmitt S, Baratte B, Koken M, Coburn SP, Tang L, Jiang T, Liang DC, Galons H, Dierick JF, Pinna LA, Meggio F, Totzke F, Schächtele C, Lerman AS, Carnero A, Wan Y, Gray N, Meijer L.** Roscovitine targets, protein kinases and pyridoxal kinase. *J Biol Chem* 280: 31208–31219, 2005. doi:10.1074/jbc.M500806200.

4. **Balat A.** Tear drops of kidney: a historical overview of Polycystic Kidney Disease. *G Ital Nefrol* 33, *Suppl* 66: 21, 2016.

5. **Bettayeb K, Baunbæk D, Delehouzé C, Loaëc N, Hole AJ, Baumli S, Endicott JA, Douc-Rasy S, Bénard J, Oumata N, Galons H, Meijer L.** CDK inhibitors roscovitine and CR8 trigger Mcl-1 down-regulation and apoptotic cell death in neuroblastoma cell lines. *Genes Cancer* 1: 369–380, 2010. doi:10.1177/1947601910369817.

6. **Bettayeb K, Oumata N, Echalier A, Ferandin Y, Endicott JA, Galons H, Meijer L.** CR8, a potent and selective, roscovitine-derived inhibitor of cyclin-dependent kinases. *Oncogene* 27: 5797–5807, 2008. doi:10.1038/onc.2008.191.

7. **Bhunia AK, Piontek K, Boletta A, Liu L, Qian F, Xu PN, Germino FJ, Germino GG.** PKD1 induces p21(waf1) and regulation of the cell cycle via direct activation of the JAK-STAT signaling pathway in a process requiring PKD2. *Cell* 109: 157–168, 2002. doi:10.1016/S0092-8674(02)00716-X.

8. **Blackburn K, Bustamante-Marin X, Yin W, Goshe MB, Ostrowski LE.** Quantitative Proteomic Analysis of Human Airway Cilia Identifies Previously Uncharacterized Proteins of High Abundance. *J Proteome Res* 16: 1579–1592, 2017. doi:10.1021/acs.jproteome.6b00912.

9. **Blair HA, Keating GM.** Tolvaptan: a review in autosomal dominant polycystic kidney disease. *Drugs* 75: 1797–1806, 2015. doi:10.1007/s40265-015-0475-x.

10. **Bloodgood RA.** From central to rudimentary to primary: the history of an underappreciated organelle whose time has come. The primary cilium. *Methods Cell Biol* 94: 3–52, 2009. doi:10.1016/S0091-679X(08)94001-2.

11. **Booij TH, Bange H, Leonhard WN, Yan K, Fokkelman M, Kunnen SJ, Dauwerse JG, Qin Y, van de Water B, van Westen GJP, Peters**

DJM, Price LS. High-throughput phenotypic screening of kinase inhibitors to identify drug targets for polycystic kidney disease. *SLAS Discov* 22: 974–984, 2017. doi:10.1177/2472555217716056.

12. **Borgal L, Rinschen MM, Dafinger C, Liebrecht VI, Abken H, Benzing T, Schermer B.** Jade-1S phosphorylation induced by CK1α contributes to cell cycle progression. *Cell Cycle* 15: 1034–1045, 2016. doi:10.1080/15384101.2016.1152429.

13. **Bukanov NO, Moreno SE, Natoli TA, Rogers KA, Smith LA, Led-better SR, Oumata N, Galons H, Meijer L, Ibraghimov-Beskrovnaya O.** CDK inhibitors R-roscovitine and S-CR8 effectively block renal and hepatic cystogenesis in an orthologous model of ADPKD. *Cell Cycle* 11: 4040–4046, 2012. doi:10.4161/cc.22375.

14. **Bukanov NO, Smith LA, Klinger KW, Ledbetter SR, Ibraghimov-Beskrovnaya O.** Long-lasting arrest of murine polycystic kidney disease with CDK inhibitor roscovitine. *Nature* 444: 949–952, 2006. doi:10.1038/nature05348.

15. **Cesaro L, Pinna LA.** The generation of phosphoserine stretches in phosphoproteins: mechanism and significance. *Mol Biosyst* 11: 2666–2679, 2015. doi:10.1039/C5MB00337G.

16. **Chen Y, Sasai N, Ma G, Yue T, Jia J, Briscoe J, Jiang J.** Sonic Hedgehog dependent phosphorylation by CK1α and GRK2 is required for ciliary accumulation and activation of smoothened. *PLoS Biol* 9: e1001083, 2011. doi:10.1371/journal.pbio.1001083.

17. **Cheng YC, Prusoff WH.** Relationship between the inhibition constant (K1) and the concentration of inhibitor which causes 50 per cent inhibition (I50) of an enzymatic reaction. *Biochem Pharmacol* 22: 3099–3108, 1973. doi:10.1016/0006-2952(73)90196-2.

18. **Choi HJ, Lin JR, Vannier JB, Slaats GG, Kile AC, Paulsen RD, Manning DK, Beier DR, Giles RH, Boulton SJ, Cimprich KA.** NEK8 links the ATR-regulated replication stress response and S phase CDK activity to renal ciliopathies. *Mol Cell* 51: 423–439, 2013. doi:10.1016/j.molcel.2013.08.006.

19. **Cicenas J, Kalyan K, Sorokinas A, Stankunas E, Levy J, Meskinyte I, Stankevicius V, Kaupinis A, Valius M.** Roscovitine in cancer and other diseases. *Ann Transl Med* 3: 135, 2015. doi:10.3978/j.issn.2305-5839.2015.03.61.

20. **Cowley BD Jr, Smardo FL Jr, Grantham JJ, Calvet JP.** Elevated c-myc protooncogene expression in autosomal recessive polycystic kidney disease [Erratum in: *Proc Natl Acad Sci USA* 85: 2578, 1988]. *Proc Natl Acad Sci USA* 84: 8394–8398, 1987. doi:10.1073/pnas.84.23.8394.

21. **Cozza G, Pinna LA.** Casein kinases as potential therapeutic targets. *Expert Opin Ther Targets* 20: 319–340, 2016. doi:10.1517/14728222.2016.1091883.

22. **Cruciat CM.** Casein kinase 1 and Wnt/β-catenin signaling. *Curr Opin Cell Biol* 31: 46–55, 2014. doi:10.1016/j.ceb.2014.08.003.

23. **Delehouzé C, Gödl K, Loaëc N, Bruyère C, Desban N, Oumata N, Galons H, Roumeliotis TI, Giannopoulou EG, Grenet J, Twitchell D, Lahti J, Mouchet N, Galibert MD, Garbis SD, Meijer L.** CDK/CK1 inhibitors roscovitine and CR8 downregulate amplified MYCN in neuroblastoma cells. *Oncogene* 33: 5675–5687, 2014. doi:10.1038/onc.2013.513.

24. **del Valle-Pérez B, Arqués O, Vinyoles M, de Herreros AG, Duñach M.** Coordinated action of CK1 isoforms in canonical Wnt signaling. *Mol Cell Biol* 31: 2877–2888, 2011. doi:10.1128/MCB.01466-10.

25. **Deng C, Lipstein MR, Scotto L, Jirau Serrano XO, Mangone MA, Li S, Vendome J, Hao Y, Xu X, Deng SX, Realubit RB, Tatonetti NP, Karan C, Lentzsch S, Fruman DA, Honig B, Landry DW, O'Connor OA.** Silencing c-Myc translation as a therapeutic strategy through targeting PI3Kδ and CK1ε in hematological malignancies. *Blood* 129: 88–99, 2017. doi:10.1182/blood-2016-08-731240.

26. **Duan S, Skaar JR, Kuchay S, Toschi A, Kanarek N, Ben-Neriah Y, Pagano M.** mTOR generates an auto-amplification loop by triggering the βTrCP- and CK1α-dependent degradation of DEPTOR. *Mol Cell* 44: 317–324, 2011. doi:10.1016/j.molcel.2011.09.005.

27. **Evangelista M, Lim TY, Lee J, Parker L, Ashique A, Peterson AS, Ye W, Davis DP, de Sauvage FJ.** Kinome siRNA screen identifies regulators of ciliogenesis and hedgehog signal transduction. *Sci Signal* 1: ra7, 2008. doi:10.1126/scisignal.1162925.

28. **Fan J, Liu Y, Jia J.** Hh-induced Smoothened conformational switch is mediated by differential phosphorylation at its C-terminal tail in a dose-and position-dependent manner. *Dev Biol* 366: 172–184, 2012. doi:10.1016/j.ydbio.2012.04.007.

29. **Fantus D, Rogers NM, Grahammer F, Huber TB, Thomson AW.** Roles of mTOR complexes in the kidney: implications for renal disease and transplantation. *Nat Rev Nephrol* 12: 587–609, 2016. doi:10.1038/nrneph.2016.108.

30. **Felekkis KN, Koupepidou P, Kastanos E, Witzgall R, Bai CX, Li L, Tsiokas L, Gretz N, Deltas C.** Mutant polycystin-2 induces proliferation in primary rat tubular epithelial cells in a STAT-1/p21-independent fashion accompanied instead by alterations in expression of p57KIP2 and Cdk2. *BMC Nephrol* 9: 10, 2008. doi:10.1186/1471-2369-9-10.

31. **Gamberi C, Hipfner DR, Trudel M, Lubell WD.** Bicaudal C mutation causes myc and TOR pathway up-regulation and polycystic kidney disease-like phenotypes in Drosophila. *PLoS Genet* 13: e1006694, 2017. doi:10.1371/journal.pgen.1006694.

32. **Gherardi D, D'Agati V, Chu TH, Barnett A, Gianella-Borradori A, Gelman IH, Nelson PJ.** Reversal of collapsing glomerulopathy in mice with the cyclin-dependent kinase inhibitor CYC202. *J Am Soc Nephrol* 15: 1212–1222, 2004. doi:10.1097/01.ASN.0000124672.41036.F4.

33. **Grampa V, Delous M, Zaidan M, Odye G, Thomas S, Elkhartoufi N, Filhol E, Niel O, Silbermann F, Lebreton C, Collardeau-Frachon S, Rouvet I, Alessandri JL, Devisme L, Dieux-Coeslier A, Cordier MP, Capri Y, Khung-Savatovsky S, Sigaudy S, Salomon R, Antignac C, Gubler MC, Benmerah A, Terzi F, Attié-Bitach T, Jeanpierre C, Saunier S.** Novel NEK8 mutations cause severe syndromic renal cystic dysplasia through YAP dysregulation. *PLoS Genet* 12: e1005894, 2016. doi:10.1371/journal.pgen.1005894.

34. **Greer YE, Westlake CJ, Gao B, Bharti K, Shiba Y, Xavier CP, Pazour GJ, Yang Y, Rubin JS.** Casein kinase 1δ functions at the centrosome and Golgi to promote ciliogenesis. *Mol Biol Cell* 25: 1629–1640, 2014. doi:10.1091/mbc.e13-10-0598.

35. **Griffin SV, Krofft RD, Pippin JW, Shankland SJ.** Limitation of podocyte proliferation improves renal function in experimental crescentic glomerulonephritis. *Kidney Int* 67: 977–986, 2005. doi:10.1111/j.1523-1755.2005.00161.x.

36. **Habbig S, Liebau MC.** Ciliopathies—from rare inherited cystic kidney diseases to basic cellular function. *Mol Cell Pediatr* 2: 8, 2015. doi:10.1186/s40348-015-0019-1.

37. **Hodeify R, Megyesi J, Tarcsafalvi A, Safirstein RL, Price PM.** Protection of cisplatin cytotoxicity by an inactive cyclin-dependent kinase. *Am J Physiol Renal Physiol* 299: F112–F120, 2010. doi:10.1152/ajprenal.00151.2010.

38. **Hodeify R, Tarcsafalvi A, Megyesi J, Safirstein RL, Price PM.** Cdk2-dependent phosphorylation of p21 regulates the role of Cdk2 in cisplatin cytotoxicity. *Am J Physiol Renal Physiol* 300: F1171–F1179, 2011. doi:10.1152/ajprenal.00507.2010.

39. **Husson H, Moreno S, Smith LA, Smith MM, Russo RJ, Pitstick R, Sergeev H, Ledbetter SR, Bukanov NO, Lane M, Zhang K, Billot K, Carlson G, Shah J, Meijer L, Beier DR, Ibraghimov-Beskrovnaya O.** Reduction of ciliary length through pharmacologic or genetic inhibition of CDK5 attenuates polycystic kidney disease in a model of nephronophthisis. *Hum Mol Genet* 25: 2245–2255, 2016. doi:10.1093/hmg/ddw093.

40. **Ibraghimov-Beskrovnaya O, Natoli TA.** mTOR signaling in polycystic kidney disease. *Trends Mol Med* 17: 625–633, 2011. doi:10.1016/j.molmed.2011.06.003.

41. **Jiang J.** CK1 in developmental signaling: Hedgehog and Wnt. *Curr Top Dev Biol* 123: 303–329, 2017. doi:10.1016/bs.ctdb.2016.09.002.

42. **Jiang K, Liu Y, Fan J, Epperly G, Gao T, Jiang J, Jia J.** Hedgehog-regulated atypical PKC promotes phosphorylation and activation of Smoothened and Cubitus interruptus in Drosophila. *Proc Natl Acad Sci USA* 111: E4842–E4850, 2014. doi:10.1073/pnas.1417147111.

43. **Kakade VR, Tao S, Rajagopal M, Zhou X, Li X, Yu AS, Calvet JP, Pandey P, Rao R.** A cAMP and CREB-mediated feed-forward mechanism regulates GSK3β in polycystic kidney disease. *J Mol Cell Biol* 8: 464–476, 2016. doi:10.1093/jmcb/mjw022.

44. **Kim HJ, Edelstein CL.** Mammalian target of rapamycin inhibition in polycystic kidney disease: From bench to bedside. *Kidney Res Clin Pract* 31: 132–138, 2012. doi:10.1016/j.krcp.2012.07.002.

45. **Kim S, Nie H, Nesin V, Tran U, Outeda P, Bai CX, Keeling J, Maskey D, Watnick T, Wessely O, Tsiokas L.** The polycystin complex mediates Wnt/Ca(2+) signalling. *Nat Cell Biol* 18: 752–764, 2016. doi:10.1038/ncb3363.

46. **Knippschild U, Krüger M, Richter J, Xu P, García-Reyes B, Peifer C, Halekotte J, Bakulev V, Bischof J.** The CK1 family: contribution to cellular stress response and its role in carcinogenesis. *Front Oncol* 4: 96, 2014. doi:10.3389/fonc.2014.00096.

47. **Knockaert M, Gray N, Damiens E, Chang YT, Grellier P, Grant K, Fergusson D, Mottram J, Soete M, Dubremetz JF, Le Roch K,**

Doerig C, Schultz P, Meijer L. Intracellular targets of cyclin-dependent kinase inhibitors: identification by affinity chromatography using immobilised inhibitors. *Chem Biol* 7: 411–422, 2000. doi:10.1016/S1074-5521(00)00124-1.

48. Kuehn EW, Walz G. Prime time for polycystic kidney disease: does one shot of roscovitine bring the cure? *Nephrol Dial Transplant* 22: 2133–2135, 2007. doi:10.1093/ndt/gfm178.

49. Kühn WE, Walz G. The treatment of autosomal dominant polycystic kidney disease. *Dtsch Arztebl Int* 112: 884–890, 2015. doi:10.3238/arztebl.2015.0884.

50. Lee KH, Johmura Y, Yu LR, Park JE, Gao Y, Bang JK, Zhou M, Veenstra TD, Yeon Kim B, Lee KS. Identification of a novel Wnt5a-CK1ε-Dvl2-Plk1-mediated primary cilia disassembly pathway. *EMBO J* 31: 3104–3117, 2012. doi:10.1038/emboj.2012.144.

51. Li A, Fan S, Xu Y, Meng J, Shen X, Mao J, Zhang L, Zhang X, Moeckel G, Wu D, Wu G, Liang C. Rapamycin treatment dose-dependently improves the cystic kidney in a new ADPKD mouse model via the mTORC1 and cell-cycle-associated CDK1/cyclin axis. *J Cell Mol Med* 21: 1619–1635, 2017. doi:10.1111/jcmm.13091.

52. Li X. *Polycystic kidney disease*. Brisbane, Australia: Codon, 2015, p. 1–488. doi:10.15586/codon.pkd.2015

53. Lin F, Hiesberger T, Cordes K, Sinclair AM, Goldstein LS, Somlo S, Igarashi P. Kidney-specific inactivation of the KIF3A subunit of kinesin-II inhibits renal ciliogenesis and produces polycystic kidney disease. *Proc Natl Acad Sci USA* 100: 5286–5291, 2003. doi:10.1073/pnas.0836980100.

54. Ma M, Tian X, Igarashi P, Pazour GJ, Somlo S. Loss of cilia suppresses cyst growth in genetic models of autosomal dominant polycystic kidney disease. *Nat Genet* 45: 1004–1012, 2013. doi:10.1038/ng.2715.

55. Malicki JJ, Johnson CA. The cilium: cellular antenna and central processing unit. *Trends Cell Biol* 27: 126–140, 2017. doi:10.1016/j.tcb.2016.08.002.

56. Maskey D, Marlin MC, Kim S, Kim S, Ong EC, Li G, Tsiokas L. Cell cycle-dependent ubiquitylation and destruction of NDE1 by CDK5-FBW7 regulates ciliary length. *EMBO J* 34: 2424–2440, 2015. doi:10.15252/embj.201490831.

57. Masyuk TV, Masyuk AI, LaRusso NF. Therapeutic targets in polycystic liver disease. *Curr Drug Targets* 18: 950–957, 2017. doi:10.2174/1389450116666150427161743.

58. Meijer L, Bettayeb K, Galons H. Roscovitine (CYC202, Seliciclib). In: *Monographs on Enzyme Inhibitors, Volume 2, CDK Inhibitors and Their Potential as Anti-Tumor Agents*, edited by Yue E and Smith PJ. Boca Raton, FL: CRC, Taylor & Francis, p. 187–226, 2006.

59. Meijer L, Nelson DJ, Riazanski V, Gabdoulkhakova AG, Hery-Arnaud G, Le Berre R, Loaëc N, Oumata N, Galons H, Nowak E, Gueganton L, Dorothée G, Prochazkova M, Hall B, Kulkarni AB, Gray RD, Rossi AG, Witko-Sarsat V, Norez C, Becq F, Ravel D, Mottier D, Rault G. Modulating innate and adaptative immunity by (R)-roscovitine: potential therapeutic opportunity in cystic fibrosis. *J Innate Immun* 8: 330–349, 2016. doi:10.1159/000444256.

60. Meijer L, Raymond E. Roscovitine and other purines as kinase inhibitors. From starfish oocytes to clinical trials. *Acc Chem Res* 36: 417–425, 2003. doi:10.1021/ar0201198.

61. Mick DU, Rodrigues RB, Leib RD, Adams CM, Chien AS, Gygi SP, Nachury MV. Proteomics of primary cilia by proximity labeling. *Dev Cell* 35: 497–512, 2015. doi:10.1016/j.devcel.2015.10.015.

62. Milovanceva-Popovska M, Kunter U, Ostendorf T, Petermann A, Rong S, Eitner F, Kerjaschki D, Barnett A, Floege J. R-roscovitine (CYC202) alleviates renal cell proliferation in nephritis without aggravating podocyte injury. *Kidney Int* 67: 1362–1370, 2005. doi:10.1111/j.1523-1755.2005.00213.x.

63. Müller S, Chaikuad A, Gray NS, Knapp S. The ins and outs of selective kinase inhibitor development. *Nat Chem Biol* 11: 818–821, 2015. doi:10.1038/nchembio.1938.

64. Ong AC, Devuyst O, Knebelmann B, Walz G; ERA-EDTA Working Group for Inherited Kidney Diseases. Autosomal dominant polycystic kidney disease: the changing face of clinical management. *Lancet* 385: 1993–2002, 2015. doi:10.1016/S0140-6736(15)60907-2.

65. Oumata N, Ferandin Y, Meijer L, Galons H. Practical synthesis of roscovitine and CR8. *Org Process Res Dev* 13: 641–644, 2009. doi:10.1021/op800284k.

66. Park JY, Park SH, Weiss RH. Disparate effects of roscovitine on renal tubular epithelial cell apoptosis and senescence: implications for autosomal dominant polycystic kidney disease. *Am J Nephrol* 29: 509–515, 2009. doi:10.1159/000184590.

67. Park JY, Schutzer WE, Lindsley JN, Bagby SP, Oyama TT, Anderson S, Weiss RH. p21 is decreased in polycystic kidney disease and leads to increased epithelial cell cycle progression: roscovitine augments p21 levels. *BMC Nephrol* 8: 12, 2007. doi:10.1186/1471-2369-8-12.

68. Pedersen LB, Mogensen JB, Christensen ST. Endocytic control of cellular signaling at the primary cilium. *Trends Biochem Sci* 41: 784–797, 2016. doi:10.1016/j.tibs.2016.06.002.

69. Pezzotta A, Mister M, Monteferrante G, Cassis L, Azzollini N, Aiello S, Satta M, Benigni A, Remuzzi G, Noris M. Effect of seliciclib (CYC202, R-roscovitine) on lymphocyte alloreactivity and acute kidney allograft rejection in rat. *Transplantation* 85: 1476–1482, 2008. doi:10.1097/TP.0b013e31816f240c.

70. Pippin JW, Qu Q, Meijer L, Shankland SJ. Direct in vivo inhibition of the nuclear cell cycle cascade in experimental mesangial proliferative glomerulonephritis with Roscovitine, a novel cyclin-dependent kinase antagonist. *J Clin Invest* 100: 2512–2520, 1997. doi:10.1172/JCI119793.

71. Price MA, Kalderon D. Proteolysis of the Hedgehog signaling effector Cubitus interruptus requires phosphorylation by Glycogen Synthase Kinase 3 and Casein Kinase 1. *Cell* 108: 823–835, 2002. doi:10.1016/S0092-8674(02)00664-5.

72. Price PM, Safirstein RL, Megyesi J. The cell cycle and acute kidney injury. *Kidney Int* 76: 604–613, 2009. doi:10.1038/ki.2009.224.

73. Price PM, Yu F, Kaldis P, Aleem E, Nowak G, Safirstein RL, Megyesi J. Dependence of cisplatin-induced cell death in vitro and in vivo on cyclin-dependent kinase 2. *J Am Soc Nephrol* 17: 2434–2442, 2006. doi:10.1681/ASN.2006020162.

74. Primot A, Baratte B, Gompel M, Borgne A, Liabeuf S, Romette JL, Jho EH, Costantini F, Meijer L. Purification of GSK-3 by affinity chromatography on immobilized axin. *Protein Expr Purif* 20: 394–404, 2000. doi:10.1006/prep.2000.1321.

75. Pronobis MI, Rusan NM, Peifer M. A novel GSK3-regulated APC: Axin interaction regulates Wnt signaling by driving a catalytic cycle of efficient βcatenin destruction. *eLife* 4: e08022, 2015. doi:10.7554/eLife.08022.

76. Rangan GK, Tchan MC, Tong A, Wong AT, Nankivell BJ. Recent advances in autosomal-dominant polycystic kidney disease. *Intern Med J* 46: 883–892, 2016. doi:10.1111/imj.13143.

77. Reinhardt J, Ferandin Y, Meijer L. Purification of CK1 by affinity chromatography on immobilised axin. *Protein Expr Purif* 54: 101–109, 2007. doi:10.1016/j.pep.2007.02.020.

78. Saigusa T, Bell PD. Molecular pathways and therapies in autosomal-dominant polycystic kidney disease. *Physiology (Bethesda)* 30: 195–207, 2015. doi:10.1152/physiol.00032.2014.

79. Santoro D, Pellicanò V, Visconti L, Trifirò G, Buemi M, Cernaro V. An overview of experimental and early investigational therapies for the treatment of polycystic kidney disease. *Expert Opin Investig Drugs* 24: 1199–1218, 2015. doi:10.1517/13543784.2015.1059421.

80. Sheryanna AM, Smith J, Bhangal G, Barnett A, McClue S, Tam FW, Cook T, Pusey CD. Treatment with a cyclin-dependent kinase inhibitor, seliciclib, is effective in reducing glomerular macrophage numbers and the severity of established experimental glomerulonephritis. *Nephrology (Carlton)* 16: 410–416, 2011. doi:10.1111/j.1440-1797.2010.01416.x.

81. Shi Q, Li S, Li S, Jiang A, Chen Y, Jiang J. Hedgehog-induced phosphorylation by CK1 sustains the activity of Ci/Gli activator. *Proc Natl Acad Sci USA* 111: E5651–E5660, 2014. doi:10.1073/pnas.1416652111.

82. Shin S, Wolgamott L, Roux PP, Yoon SO. Casein kinase 1ε promotes cell proliferation by regulating mRNA translation. *Cancer Res* 74: 201–211, 2014. doi:10.1158/0008-5472.CAN-13-1175.

83. Streets AJ, Moon DJ, Kane ME, Obara T, Ong AC. Identification of an N-terminal glycogen synthase kinase 3 phosphorylation site which regulates the functional localization of polycystin-2 in vivo and in vitro. *Hum Mol Genet* 15: 1465–1473, 2006. doi:10.1093/hmg/ddl070.

84. Tao S, Kakade VR, Woodgett JR, Pandey P, Suderman ED, Rajagopal M, Rao R. Glycogen synthase kinase-3β promotes cyst expansion in polycystic kidney disease. *Kidney Int* 87: 1164–1175, 2015. doi:10.1038/ki.2014.427.

85. Tobin JL, Beales PL. Restoration of renal function in zebrafish models of ciliopathies. *Pediatr Nephrol* 23: 2095–2099, 2008. doi:10.1007/s00467-008-0898-7.

86. Tran PV, Haycraft CJ, Besschetnova TY, Turbe-Doan A, Stottmann RW, Herron BJ, Chesebro AL, Qiu H, Scherz PJ, Shah JV, Yoder

BK, Beier DR. THM1 negatively modulates mouse sonic hedgehog signal transduction and affects retrograde intraflagellar transport in cilia. *Nat Genet* 40: 403–410, 2008. doi:10.1038/ng.105.

87. **Tran PV, Talbott GC, Turbe-Doan A, Jacobs DT, Schonfeld MP, Silva LM, Chatterjee A, Prysak M, Allard BA, Beier DR.** Downregulating hedgehog signaling reduces renal cystogenic potential of mouse models. *J Am Soc Nephrol* 25: 2201–2212, 2014. doi:10.1681/ASN.2013070735.

88. **Trudel M.** c-Myc Signalling in the genetic mechanism of polycystic kidney disease. In: *Polycystic Kidney Disease*, edited by Li X. Brisbane, Australia: Codon; 2015.

89. **Trudel M, Barisoni L, Lanoix J, D'Agati V.** Polycystic kidney disease in SBM transgenic mice: role of c-myc in disease induction and progression. *Am J Pathol* 152: 219–229, 1998.

90. **Trudel M, D'Agati V, Costantini F.** C-myc as an inducer of polycystic kidney disease in transgenic mice. *Kidney Int* 39: 665–671, 1991. doi:10.1038/ki.1991.80.

91. **van Kappel EC, Maurice MM.** Molecular regulation and pharmacological targeting of the β-catenin destruction complex. *Br J Pharmacol* 174: 4575–4588, 2017. doi:10.1111/bph.13922.

92. **Wu M, Yang C, Tao B, Bu S, Guay-Woodford LM.** The ciliary protein cystin forms a regulatory complex with necdin to modulate Myc expression. *PLoS One* 8: e83062, 2013. doi:10.1371/journal.pone.0083062.

93. **Wu P, Clausen MH, Nielsen TE.** Allosteric small-molecule kinase inhibitors. *Pharmacol Ther* 156: 59–68, 2015. doi:10.1016/j.pharmthera.2015.10.002.

94. **Wu P, Nielsen TE, Clausen MH.** Small-molecule kinase inhibitors: an analysis of FDA-approved drugs. *Drug Discov Today* 21: 5–10, 2016. doi:10.1016/j.drudis.2015.07.008.

95. **Wu P, Nielsen TE, Clausen MH.** FDA-approved small-molecule kinase inhibitors. *Trends Pharmacol Sci* 36: 422–439, 2015. doi:10.1016/j.tips.2015.04.005.

96. **Ye LC, Jiang C, Bai J, Jiang J, Hong HF, Qiu LS.** Knockdown of casein kinase 1ε inhibits cell proliferation and invasion of colorectal cancer cells via inhibition of the Wnt/β-catenin signaling. *J Biol Regul Homeost Agents* 29: 307–315, 2015.

97. **Zhou JX, Fan LX, Li X, Calvet JP, Li X.** TNFα signaling regulates cystic epithelial cell proliferation through Akt/mTOR and ERK/MAPK/Cdk2 mediated Id2 signaling. *PLoS One* 10: e0131043, 2015. doi:10.1371/journal.pone.0131043.

98. **Zhou Q, Kalderon D.** Hedgehog activates fused through phosphorylation to elicit a full spectrum of pathway responses. *Dev Cell* 20: 802–814, 2011. doi:10.1016/j.devcel.2011.04.020.

99. **Zhu P, Sieben CJ, Xu X, Harris PC, Lin X.** Autophagy activators suppress cystogenesis in an autosomal dominant polycystic kidney disease model. *Hum Mol Genet* 26: 158–172, 2017. doi:10.1093/hmg/ddw376.

100. **Zoja C, Casiraghi F, Conti S, Corna D, Rottoli D, Cavinato RA, Remuzzi G, Benigni A.** Cyclin-dependent kinase inhibition limits glomerulonephritis and extends lifespan of mice with systemic lupus. *Arthritis Rheum* 56: 1629–1637, 2007. doi:10.1002/art.22593.